

# Shape-Function Effects and Split Matching in $B \rightarrow X_s \ell^+ \ell^-$

Keith S. M. Lee and Iain W. Stewart

*Center for Theoretical Physics, Laboratory for Nuclear Science,  
Massachusetts Institute of Technology, Cambridge, MA 02139\**

## Abstract

We derive the triply differential spectrum for the inclusive rare decay  $B \rightarrow X_s \ell^+ \ell^-$  in the shape function region, in which  $X_s$  is jet-like with  $m_X^2 \lesssim m_b \Lambda_{\text{QCD}}$ . Experimental cuts make this a relevant region. The perturbative and non-perturbative parts of the matrix elements can be defined with the Soft-Collinear Effective Theory, which is used to incorporate  $\alpha_s$  corrections consistently. We show that, with a suitable power counting for the dilepton invariant mass, the same universal jet and shape functions appear as in  $B \rightarrow X_s \gamma$  and  $B \rightarrow X_u \ell \bar{\nu}$  decays. Parts of the usual  $\alpha_s(m_b)$  corrections go into the jet function at a lower scale, and parts go into the non-perturbative shape function. For  $B \rightarrow X_s \ell^+ \ell^-$ , the perturbative series in  $\alpha_s$  are of a different character above and below  $\mu = m_b$ . We introduce a “split matching” method that allows the series in these regions to be treated independently.

arXiv:hep-ph/0511334v2 10 Jan 2006

---

\* Electronic address: ksml@mit.edu, iains@mit.edu

## I. INTRODUCTION

The  $B$  meson is particularly suitable for probing QCD and flavor physics in the Standard Model, since the large mass of the  $b$  quark relative to  $\Lambda_{\text{QCD}}$  provides a useful expansion parameter,  $\Lambda_{\text{QCD}}/m_b \sim 0.1$ . The study of inclusive  $B$  decays circumvents the need for precision hadronic form factors, while still allowing model-independent predictions. Rare inclusive decays, which involve flavor-changing neutral currents (FCNCs), not only allow measurements of CKM matrix elements, in particular  $V_{ts}$  and  $V_{td}$ , but are also highly sensitive to new physics, since they do not occur at tree level in the Standard Model.

Among the inclusive rare  $B$  decays, the radiative process  $B \rightarrow X_s \gamma$  has received the most attention, having been measured first by CLEO [1] and subsequently by other experiments [2, 3, 4, 5]. These measurements have provided significant constraints on extensions to the Standard Model. The decay  $B \rightarrow X_s \ell^+ \ell^-$  is complementary to, and more complicated than,  $B \rightarrow X_s \gamma$ . Its potential for revealing information beyond that supplied by the radiative decay is due to the presence of two extra operators in the effective electroweak Hamiltonian and the availability of additional kinematical variables, such as the dilepton invariant-mass spectrum and the forward-backward asymmetry. Belle and BABAR have already made initial measurements of this dilepton process [6, 7].

Provided that one makes suitable phase-space cuts to avoid  $c\bar{c}$  resonances,  $B \rightarrow X_s \ell^+ \ell^-$  is dominated by the quark-level process, which was calculated in Ref. [8]. Owing to the disparate scales,  $m_b \ll m_W$ , one encounters large logarithms of the form  $\alpha_s^n(m_b) \log^n(m_b/m_W)$  (leading log [LL]),  $\alpha_s^{n+1}(m_b) \log^n(m_b/m_W)$  (next-to-leading log [NLL]),  $\dots$ , which should be summed. The NLL calculations were completed in Refs. [9, 10], and the NNLL analysis, although technically not fully complete, is at a level that the scale uncertainties have been substantially reduced, after the combined efforts of a number of groups [11, 12, 13, 14, 15].

Non-perturbative corrections to the quark-level result can also be calculated by means of a local operator product expansion (OPE) [16], with non-perturbative matrix elements defined with the help of the Heavy Quark Effective Theory (HQET) [17]. As is the case for  $B \rightarrow X_s \gamma$  and  $B \rightarrow X_u \ell \bar{\nu}$ , there are no  $\mathcal{O}(1/m_b)$  corrections. The  $\mathcal{O}(1/m_b^2)$  corrections and OPE were considered in Ref. [18] and subsequently corrected in Ref. [19]. The  $\mathcal{O}(1/m_b^3)$  corrections were computed in Ref. [20]. There are also non-perturbative contributions arising from the  $c\bar{c}$  intermediate states. The largest  $c\bar{c}$  resonances, i.e. the  $J/\psi$  and  $\psi'$ , can be removed by suitable cuts in the dilepton mass spectrum. It is generally believed that the operator product expansion holds for the computation of the dilepton invariant mass as long as one avoids the region with the first two narrow resonances, although no complete proof of this (for the full operator basis) has been given. A picture for the structure of resonances can be obtained using the model of Krüger and Sehgal [21], which estimates factorizable contributions based on a dispersion relation and experimental data on  $\sigma(e^+e^- \rightarrow c\bar{c} + \text{hadrons})$ . Non-factorizable effects have been estimated in a model-independent way by means of an expansion in  $1/m_c$  [22], which is valid only away from the resonances.

Staying away from the resonance regions in the dilepton mass spectrum leaves two perturbative windows, the low- and high- $q^2$  regions, corresponding to  $q^2 \leq 6 \text{ GeV}^2$  and  $q^2 \geq 14.4 \text{ GeV}^2$  respectively. These have complementary advantages and disadvantages [15]. For example, the latter has significant  $1/m_b$  corrections but negligible scale and charm-mass dependence, whereas the former has small  $1/m_b$  corrections but non-negligible scale and charm-mass dependence. The low- $q^2$  region has a high rate compared to the high- $q^2$  region and so experimental spectra will become precise for this region first. However, at low  $q^2$

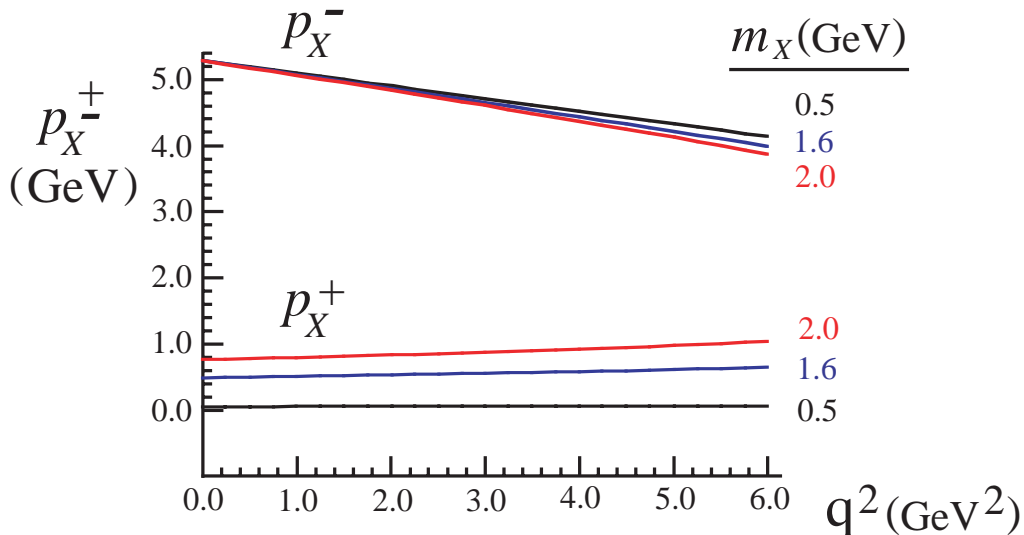


FIG. 1: The kinematic range for  $p_X^-$  and  $p_X^+$  given the experimental cuts of  $q^2 < 6 \text{ GeV}^2$  and  $m_X \leq 2.0 \text{ GeV}$  for  $B \rightarrow X_s \ell^+ \ell^-$ .

an additional cut is required, making measurements less inclusive. In particular, a hadronic invariant-mass cut is imposed in order to eliminate the combinatorial background, which includes the semileptonic decay  $b \rightarrow c (\rightarrow s e^+ \nu) e^- \bar{\nu} = b \rightarrow s e^+ e^- + \text{missing energy}$ . The latest analyses from *BABAR* and *Belle* impose cuts of  $m_X \leq 1.8 \text{ GeV}$  and  $m_X \leq 2.0 \text{ GeV}$  respectively [23], which in the  $B$ -meson rest frame correspond to  $q^0 \gtrsim 2.3 \text{ GeV}$ . This cut dependence has so far been analyzed only in the Fermi-motion model [24], and not in a model-independent formalism.

When  $m_X^2 \lesssim m_b \Lambda$ , the operator product expansion must be rearranged, and, instead of depending on non-perturbative parameters ( $\lambda_1, \lambda_2, \dots$ ) that are matrix elements of local operators, the decay rates depend on non-perturbative functions. In this so-called shape function region, the set of outgoing hadronic states becomes more jet-like and the relevant degrees of freedom are collinear and ultrasoft modes. The appropriate theoretical method is then the Soft-Collinear Effective Theory (SCET) [25, 26, 27, 28]. The endpoint region has been the focus of much work in the context of  $B \rightarrow X_s \gamma$  and  $B \rightarrow X_u \ell \bar{\nu}$  (see e.g. Refs. [28, 29, 30, 31, 32, 33, 34, 35, 36, 37, 38, 39, 40, 41, 42]). In  $B \rightarrow X_u \ell \bar{\nu}$  this is because of the cuts used to eliminate the dominant  $b \rightarrow c$  background. In  $B \rightarrow X_s \gamma$ , it is known that cuts with  $q^0 \gtrsim 2.1 \text{ GeV}$  put us in the shape function region.<sup>1</sup> In the small- $q^2$  region of  $B \rightarrow X_s \ell^+ \ell^-$  with  $q^0 \geq 2.3 \text{ GeV}$ , shape-function effects also dominate rather than the expansion in local operators. To see this, note that the cut causes  $2m_B E_X = m_B^2 + m_X^2 - q^2 \gg m_X^2$ . Decomposing  $2E_X = p_X^+ + p_X^-$  with  $m_X^2 = p_X^- p_X^+$ , we see that the  $X_s$  is jet-like with  $p_X^- \gg p_X^+$ , and the restricted sum over states in the  $X_s$  causes the non-perturbative shape functions to become important. For the experimental cuts on  $q^2$  and  $m_X$ , values for  $p_X^\pm$  are shown in

<sup>1</sup> In Ref. [43] it was pointed out that even a cut of  $E_\gamma \geq E_0 = 1.8 \text{ GeV}$ , corresponding to  $m_X \lesssim 3 \text{ GeV}$ , might not guarantee that a theoretical description in terms of the local OPE is sufficient, owing to sensitivity to the scale  $\Delta = m_b - 2E_0$  in power and perturbative corrections. Using a multi-scale OPE with an expansion in  $\Lambda/\Delta$  allows the shape function and local OPE regions to be connected [32, 33, 43].

Fig. 1.

Here we study  $B \rightarrow X_s \ell^+ \ell^-$  ( $\ell = e, \mu$ ) in the shape function region, where the relevant scales are  $m_W^2 \gg m_b^2 \gg m_b \Lambda_{\text{QCD}} \gg \Lambda_{\text{QCD}}^2$ . In this paper, we work out theoretical expressions for the triply differential decay rate, incorporating the leading shape function and a proper treatment of the perturbative corrections at each of these scales. Implications for relating the  $B \rightarrow X_s \ell^+ \ell^-$  measurements with the  $m_X$  cut to the Wilson coefficients are presented in a companion publication [44].

To compute  $B \rightarrow X_s \ell^+ \ell^-$  in the shape function region with renormalization-group evolution requires the following steps:

- i) matching the Standard Model at  $\mu \simeq m_W$  on to  $H_W$ ,
- ii) running  $H_W$  to  $\mu \simeq m_b$ ,
- iii) matching at  $\mu \simeq m_b$  on to operators in SCET,
- iv) running in SCET to  $\mu \simeq \sqrt{m_b \Lambda}$ ,
- v) computation of the imaginary part of forward-scattering time-ordered products in SCET at  $\mu \simeq \sqrt{m_b \Lambda}$ . This leads to a separation of scales in a factorization theorem, which at LO takes the form

$$d^3\Gamma^{(0)} = H \int dk \mathcal{J}(k) f^{(0)}(k),$$

with perturbative  $H$  and  $\mathcal{J}$ , and the LO non-perturbative shape function  $f^{(0)}$ ,

- vi) evolution of the shape function  $f^{(0)}$  from  $\Lambda_{\text{QCD}}$  up to  $\mu \simeq \sqrt{m_b \Lambda_{\text{QCD}}}$ .

A major part of our analysis involves step iii). This links the results in steps i-ii), which are known from the local OPE for  $B \rightarrow X_s \ell^+ \ell^-$ , with the endpoint analysis in iv-vi), which is similar to that for other inclusive processes. Note that the operator product expansion in v) occurs at  $\mu \simeq \sqrt{m_b \Lambda}$ , rather than at  $m_b^2$ , as in the standard local OPE. In step iv) we run the hard functions down using results from Refs. [25, 26]. In step vi) we run the shape function up to the intermediate scale using the simple result from Ref. [33]. An equally valid option would be to evolve the perturbative parts of the rate down to a scale  $\mu \simeq 1 \text{ GeV}$ , as considered earlier [25, 32, 45].

Each of the steps i)-vi) gives a piece of the total decay rate. At leading order in the power expansion it takes the schematic form

$$d^3\Gamma^{(0)} = \mathcal{E}(\mu_W) U_W(\mu_W, \mu_0) \mathcal{B}(\mu_0) U_H(\mu_0, \mu_i) \mathcal{J}(\mu_i) U_S(\mu_i, \mu_\Lambda) f^{(0)}(\mu_\Lambda),$$

$$\mu_W \simeq m_W, \quad \mu_0 \simeq m_b, \quad \mu_i \simeq (m_b \Lambda)^{1/2}, \quad \mu_\Lambda \simeq 1 \text{ GeV}, \quad (1)$$

where  $\mathcal{E}$ ,  $\mathcal{B}$  and  $\mathcal{J}$  represent matching at various scales, and  $U_W$ ,  $U_H$  and  $U_S$  represent the running between these scales. Eq. (1) shows only the scale dependence explicitly, not the kinematic dependences or the convolutions between  $\mathcal{J}$ ,  $U_S$ , and  $f^{(0)}$ , which we describe later on.

In Eq. (1), the order of the resummed analysis (LL, NLL, NNLL, etc.) above and below  $\mu \simeq m_b$  appears to be tied together. Above  $\mu \simeq m_b$  the series of  $(\alpha_s \ln)^k$  terms are of the standard form, with a basis of  $\sim 10$  operators, and in  $B \rightarrow X_s \ell^+ \ell^-$  their mixing is

crucial. Below  $\mu \simeq m_b$  the evolution is universal for all leading-order operators, but there are Sudakov double logarithms of the ratios of scales, which give a more complicated series. It turns out to be convenient to decouple these two stages of resummation so that one can consider working to different orders in the  $\alpha_s$  expansion above and below  $\mu = m_b$ . There is a simple reason why this decoupling is important: for  $\mu \geq m_b$  the power counting and running are for currents in the electroweak Hamiltonian and dictate treating  $C_9 \sim 1/\alpha_s$  with  $C_7 \sim 1$  and  $C_{10} \sim 1$ . However, at  $\mu = m_b$  the coefficients  $C_9$  and  $C_{10}$  are numerically comparable. For  $\mu \leq m_b$  in the shape function region we must organize the power counting and running for time-ordered products of currents in SCET rather than amplitudes, and it would be vexing to have to include terms  $\propto C_9^2$  to  $\mathcal{O}(\alpha_s^2)$  before including the  $C_{10}^2$  and  $C_7^2$  terms. Once we are below the scale  $m_b$  a counting with  $C_9 \sim C_{10} \sim C_7 \sim 1$  is more appropriate.

To decouple these two regions for  $B \rightarrow X_s \ell^+ \ell^-$  decays we make use of two facts: i) for  $\mu \geq m_b$  the operator  $\mathcal{O}_{10}$  involves a conserved current and has no operators mixing into it, so it does not have an anomalous dimension, and ii) for  $\mu \leq m_b$  all LO operators in the Soft-Collinear Effective Theory have the same anomalous dimension [26]. These properties ensure that we can separate the perturbative treatments in these two regions at any order in perturbation theory. This is done by introducing two matching scales,  $\mu_0 \simeq m_b$  and  $\mu_b \simeq m_b$ . The two aforementioned facts allow us to write

$$\begin{aligned} U_W(\mu_W, \mu_0) \mathcal{B}(\mu_0) U_H(\mu_0, \mu_i) &= U_W(\mu_W, \mu_0) \mathcal{B}(\mu_0, \mu_b) U_H(\mu_b, \mu_i) \\ &= U_W(\mu_W, \mu_0) B_1(\mu_0) B_2(\mu_b) U_H(\mu_b, \mu_i), \end{aligned} \quad (2)$$

with well-defined  $B_1$  and  $B_2$  to all orders in perturbation theory. We define  $B_2(\mu_b)$  by using the matching for the operator  $\mathcal{O}_{10}$  and extend this to find  $B_2$  matching coefficients for the other operators using property ii) above. The remaining contributions match on to  $B_1$ . Diagrams which are related to the anomalous dimension for  $\mu \geq m_b$  end up being matched at the scale  $\mu_0$  on to  $B_1$ , while those related to anomalous dimensions for  $\mu \leq m_b$  are matched at a different scale,  $\mu_b$ , on to  $B_2$ . This leaves

$$d^3\Gamma^{(0)} = \left[ \mathcal{E}(\mu_W) U_W(\mu_W, \mu_0) B_1(\mu_0) \right] \left[ B_2(\mu_b) U_H(\mu_b, \mu_i) \mathcal{J}(\mu_i) U_S(\mu_i, \mu_\Lambda) f^{(0)}(\mu_\Lambda) \right], \quad (3)$$

which is the product of two pieces that are separately  $\mu$ -independent. We refer to this procedure as “split matching” because formally we match diagrams at two scales rather than at a single scale. The two matching  $\mu$ 's are “split” because they are parametrically similar in the power-counting sense.

We organize the remainder of our paper in a manner that reflects the steps outlined above. Step iii) determines the hard matching functions,  $\mathcal{B} = B_1 B_2$ , for  $B \rightarrow X_s \ell^+ \ell^-$  in SCET, which is one of the main points of our paper. This matching is discussed in Sec. II A at leading power and one-loop order (including both bottom-, charm-, and light-quark loops and other virtual corrections). The extension to higher orders is also illustrated. Steps i) and ii) are the same as for the local OPE, so the known results can be taken over and are summarized in Sec. II A, together with Appendix A. In Sec. II B we review the universal running for step iv), which is identical to  $B \rightarrow X_u \ell \bar{\nu}$ . In Sec. II C, we discuss the basic ingredients for the triply differential decay rate and the forward-backward asymmetry in terms of hadronic tensors. The SCET matrix-element computation, step v), is performed in Sec. II D, where the leading shape function and jet function are defined. In Sec. II E we review the running for the shape function, step vi). In Sec. III we present our results for the differential decay

rates at leading order in the power expansion, including all the ingredients from Sec. II and incorporating the relevant experimental cuts. The triply differential spectrum and doubly differential spectra are discussed here in subsections IIIA-D. Readers interested only in the final results may skip directly to these sections. We compare numerical results for matching coefficients at  $m_b$  with terms in the local OPE in Sec. III E. In Appendix B we briefly comment on how our analysis will change if we assume a parametrically small dilepton invariant mass,  $q^2 \sim \lambda^2$ , rather than the generic scaling  $q^2 \sim \lambda^0$  assumed in the body of the paper. (For the case  $q^2 \sim \lambda^2$ , the rate for  $B \rightarrow X_s \ell \ell$  would *not* be determined by a factorization theorem with the same structure as for  $B \rightarrow X_u \ell \bar{\nu}$ .)

## II. ANALYSIS IN THE SHAPE FUNCTION REGION

### A. Matching on to SCET

We begin by reviewing the form of the electroweak Hamiltonian obtained after evolution down to the scale  $\mu \simeq m_b$ , and then perform the leading-order matching of this Hamiltonian on to operators in SCET. For the treatment of  $\gamma_5$  we use the NDR scheme throughout. Below the scale  $\mu = m_W$ , the effective Hamiltonian for  $b \rightarrow s \ell^+ \ell^-$  takes the form [8]

$$\mathcal{H}_W = -\frac{4G_F}{\sqrt{2}} V_{tb} V_{ts}^* \sum_{i=1}^{10} C_i(\mu) \mathcal{O}_i(\mu), \quad (4)$$

where we have used unitarity of the CKM matrix to remove  $V_{cb} V_{cs}^*$  dependence and have neglected the tiny  $V_{ub} V_{us}^*$  terms. The operators  $\mathcal{O}_i(\mu)$  are

$$\begin{aligned} \mathcal{O}_1 &= (\bar{s}_{L\alpha} \gamma_\mu b_{L\beta}) (\bar{c}_{L\beta} \gamma^\mu c_{L\alpha}), & \mathcal{O}_2 &= (\bar{s}_{L\alpha} \gamma_\mu b_{L\alpha}) (\bar{c}_{L\beta} \gamma^\mu c_{L\beta}), & (5) \\ \mathcal{O}_3 &= (\bar{s}_{L\alpha} \gamma_\mu b_{L\alpha}) \sum_{q=u,d,s,c,b} (\bar{q}_{L\beta} \gamma^\mu q_{L\beta}), & \mathcal{O}_4 &= (\bar{s}_{L\alpha} \gamma_\mu b_{L\beta}) \sum_{q=u,d,s,c,b} (\bar{q}_{L\beta} \gamma^\mu q_{L\alpha}), \\ \mathcal{O}_5 &= (\bar{s}_{L\alpha} \gamma_\mu b_{L\alpha}) \sum_{q=u,d,s,c,b} (\bar{q}_{R\beta} \gamma^\mu q_{R\beta}), & \mathcal{O}_6 &= (\bar{s}_{L\alpha} \gamma_\mu b_{L\beta}) \sum_{q=u,d,s,c,b} (\bar{q}_{R\beta} \gamma^\mu q_{R\alpha}), \\ \mathcal{O}_7 &= \frac{e}{16\pi^2} \bar{s} \sigma_{\mu\nu} F^{\mu\nu} (\bar{m}_b P_R + \bar{m}_s P_L) b, & \mathcal{O}_8 &= \frac{g}{16\pi^2} \bar{s}_\alpha T_{\alpha\beta}^a \sigma_{\mu\nu} (\bar{m}_b P_R + \bar{m}_s P_L) b_\beta G^{a\mu\nu}, \\ \mathcal{O}_9 &= \frac{e^2}{16\pi^2} \bar{s}_{L\alpha} \gamma^\mu b_{L\alpha} \bar{\ell} \gamma_\mu \ell, & \mathcal{O}_{10} &= \frac{e^2}{16\pi^2} \bar{s}_{L\alpha} \gamma^\mu b_{L\alpha} \bar{\ell} \gamma_\mu \gamma_5 \ell, \end{aligned}$$

where  $P_{R,L} = (1 \pm \gamma_5)/2$ . In the following, we shall neglect the mass of the strange quark in  $\mathcal{O}_{7,8}$ . For our analysis,  $m_s$  is not needed as a regulator for IR divergences, which are explicitly cut off by non-perturbative scales  $\sim \Lambda_{\text{QCD}}$ . In the shape function region, the  $m_s$ -quark-mass dependence is small and was computed in Ref. [46]. Non-perturbative sensitivity to  $m_s$  shows up only at subleading power, while computable  $\mathcal{O}(m_s^2/m_b \Lambda_{\text{QCD}})$  jet-function corrections are numerically smaller than the  $\Lambda_{\text{QCD}}/m_b$  power corrections.

At NLL order, one requires the NLL Wilson coefficient of  $\mathcal{O}_9$  and the LL coefficients of

the other operators. For  $\mathcal{O}_{7,9,10}$  these are given by [9, 10]

$$\begin{aligned}
C_7^{\text{NDR}}(\mu) &= r_0^{-\frac{16}{23}} C_7(M_W) + \frac{8}{3} \left( r_0^{-\frac{14}{23}} - r_0^{-\frac{16}{23}} \right) C_8(M_W) + \sum_{i=1}^8 t_i r_0^{-a_i}, \\
C_9^{\text{NDR}}(\mu) &= P_0^{\text{NDR}}(\mu) + \frac{Y(m_t^2/M_W^2)}{\sin^2 \theta_W} - 4Z(m_t^2/M_W^2) + P_E(\mu)E(m_t^2/M_W^2), \\
C_{10}(\mu) &= C_{10}(M_W) = -\frac{Y(m_t^2/M_W^2)}{\sin^2 \theta_W},
\end{aligned} \tag{6}$$

where  $C_7(m_W)$ ,  $C_8(m_W)$  and the Inami-Lim functions  $Y$ ,  $Z$ , and  $E$  are obtained from matching at  $\mu = m_W$ , and are given in Appendix A. The  $\mu$ -dependent factors include [9, 10]

$$\begin{aligned}
P_0^{\text{NDR}}(\mu) &= \frac{\pi}{\alpha_s(M_W)} \left( -0.1875 + \sum_{i=1}^8 p_i r_0^{-a_i-1} \right) + 1.2468 + \sum_{i=1}^8 r_0^{-a_i} (\rho_i^{\text{NDR}} + s_i r_0^{-1}), \\
P_E(\mu) &= 0.1405 + \sum_{i=1}^8 q_i r_0^{-a_i-1}, \quad r_0 = \frac{\alpha_s(\mu)}{\alpha_s(m_W)}.
\end{aligned} \tag{7}$$

The numbers  $t_i$ ,  $a_i$ ,  $\rho_i^{\text{NDR}}$ ,  $s_i$ ,  $q_i$  that appear here are listed in Appendix A. Results for the running coefficients of the four-quark operators,  $C_{1-6}(\mu)$ , can be found in Ref. [9]. We have modified the standard notation slightly (e.g.  $r_0(\mu)$ ) to conform with additional stages of the RG evolution discussed in sections II B and II E. Contributions beyond NLL will be mentioned below.

At a scale  $\mu \approx m_b$ , we need to match  $b \rightarrow s\ell^+\ell^-$  matrix elements of  $\mathcal{H}_W$  on to matrix elements of operators in SCET with a power expansion in the small parameter  $\lambda$ , where  $\lambda^2 = \Lambda_{\text{QCD}}/m_b$ . For convenience, we refer to the resulting four-fermion scalar operators in SCET as ‘‘currents’’ and use the notation  $J_{\ell\ell}$ . In SCET we also need the effective Lagrangians. The heavy quark in the initial state is matched on to an HQET field  $h_v$ , and the light energetic strange quark is matched on to a collinear field  $\xi_n$ . For the leading-order analysis in  $\Lambda/m_b$  we need only the lowest-order terms,

$$\mathcal{H}_W = -\frac{G_F \alpha}{\sqrt{2}\pi} (V_{tb} V_{ts}^*) J_{\ell\ell}^{(0)}, \quad \mathcal{L} = \mathcal{L}_{\text{HQET}}^{(0)} + \mathcal{L}_{\text{SCET}}^{(0)}, \tag{8}$$

where  $J_{\ell\ell}^{(0)}$  is the LO operator and the quark contributions to the HQET and SCET actions are

$$\begin{aligned}
\mathcal{L}_{\text{HQET}}^{(0)} &= \bar{h}_v i v \cdot D_{us} h_v, \\
\mathcal{L}_{\text{SCET}}^{(0)} &= \bar{\xi}_n \left[ i n \cdot D_c + i \not{D}_c^\perp \frac{1}{i \bar{n} \cdot D_c} i \not{D}_c^\perp \right] \frac{\not{n}}{2} \xi_n.
\end{aligned} \tag{9}$$

The covariant derivatives  $D_{us}$  and  $D_c$  involve ultrasoft and collinear gluons respectively, and we have made a field redefinition on the collinear fields to decouple the ultrasoft gluons at LO [28]. For convenience, we define the objects

$$\begin{aligned}
\mathcal{H}_v &= Y^\dagger h_v, & \psi_{us} &= Y^\dagger q_{us}, & \mathcal{D}_{us} &= Y^\dagger D_{us} Y \\
\chi_n &= W^\dagger \xi_n, & \mathcal{D}_c &= W^\dagger D_c W, & i g \mathcal{B}_c^\mu &= \left[ \frac{1}{\mathcal{P}} W^\dagger [i \bar{n} \cdot D_c, i D_c^\mu] W \right],
\end{aligned} \tag{10}$$

which contain ultrasoft and collinear Wilson lines,

$$Y(x) = P \exp \left( ig \int_{-\infty}^0 ds n \cdot A_{us}(x+ns) \right) \quad (11)$$

and

$$W(x) = P \exp \left( ig \int_{-\infty}^0 ds \bar{n} \cdot A_n(x+s\bar{n}) \right), \quad (12)$$

as well as the label operator  $\bar{\mathcal{P}}$  [27].

To simplify the analysis we treat both  $m_c$  and  $m_b$  as hard scales and integrate out both charm and bottom loops at  $\mu \simeq m_b$ . At leading order in SCET, the currents that we match on to are

$$\begin{aligned} J_{\ell\ell}^{(0)} = & \sum_{i=a,b,c} C_{9i}(s) (\bar{\chi}_{n,p} \Gamma_i^{(v)\mu} \mathcal{H}_v) (\bar{\ell} \gamma_\mu \ell) + \sum_{i=a,b,c} C_{10i}(s) (\bar{\chi}_{n,p} \Gamma_i^{(v)\mu} \mathcal{H}_v) (\bar{\ell} \gamma_\mu \gamma_5 \ell) \\ & - \sum_{j=a,\dots,d} C_{7j}(s) 2m_B (\bar{\chi}_{n,p} \Gamma_j^{(t)\mu} \mathcal{H}_v) (\bar{\ell} \gamma_\mu \ell), \end{aligned} \quad (13)$$

where the sum is over Dirac structures to be discussed below. In Eq. (13) two auxiliary four-vectors appear,  $v^\mu$  and  $n^\mu$ . The  $B$  momentum, total momentum of the leptons, and jet momentum (sum of the four-momenta of all the hadrons in  $X_s$ ) are

$$p_B^\mu = m_B v^\mu, \quad q^\mu = p_{\ell^+}^\mu + p_{\ell^-}^\mu, \quad p_X^\mu = n \cdot p_X \frac{\bar{n}^\mu}{2} + \bar{n} \cdot p_X \frac{n^\mu}{2}, \quad (14)$$

respectively. Here  $v^2 = 1$  and  $n^\mu$  and  $\bar{n}^\mu$  are light-like vectors, which satisfy  $n^2 = \bar{n}^2 = 0$  and  $n \cdot \bar{n} = 2$ . The components of a vector can then be written as  $(p^+, p^-, p_\perp) = (n \cdot p, \bar{n} \cdot p, p_\perp^\mu)$ . We use a frame in which  $q_\perp^\mu = v_\perp^\mu = 0$  and  $v^\mu = (n^\mu + \bar{n}^\mu)/2$ . Since  $p_X = m_B v - q$  we have

$$\begin{aligned} p_X^2 = m_X^2 = & \bar{n} \cdot p_X n \cdot p_X = m_B^2 + q^2 - m_B (n \cdot q + \bar{n} \cdot q), \quad q^2 = \bar{n} \cdot q n \cdot q, \\ \bar{n} \cdot p_X = & m_B - \bar{n} \cdot q, \quad n \cdot p_X = m_B - n \cdot q. \end{aligned} \quad (15)$$

For later convenience we define the hadronic dimensionless variables

$$x_H = \frac{2E_{\ell^-}}{m_B}, \quad \bar{y}_H = \frac{\bar{n} \cdot p_X}{m_B}, \quad u_H = \frac{n \cdot p_X}{m_B}, \quad y_H = \frac{q^2}{m_B^2}. \quad (16)$$

In SCET the total partonic  $\bar{n} \cdot p$  momentum of the jet is a hard momentum  $\sim m_b$  and also appears in the SCET Wilson coefficients. At LO,  $\bar{n} \cdot p = (m_b^2 - q^2)/m_b$  and demanding that  $\bar{n} \cdot p$  is large means only that  $q^2$  cannot be too close to  $m_b^2$ . For example, neither  $q^2 \approx 0$  nor  $q^2 \approx m_b^2/2$  modifies the power counting for  $\bar{n} \cdot p$ . Thus, there is no requirement to impose a scaling that  $q^2$  be small. For convenience, in the hard coefficients we write

$$C(\bar{n} \cdot p, m_b, \mu_0, \mu_b) \rightarrow C(s, m_b, \mu_0, \mu_b), \quad s = \frac{q^2}{m_b^2}, \quad (17)$$

since the partonic variable  $s$  is a more natural choice in  $b \rightarrow s \ell^+ \ell^-$  and is equivalent at LO. For purposes of power counting in this paper we count  $s \sim \lambda^0$ . We shall see in section III E

that varying  $s$  causes a very mild change in the coefficients. In Appendix B we briefly explore a different scenario, in which  $s \sim \lambda^2$ . A distinction between two matching scales  $\mu_0$  and  $\mu_b$  is made in  $C$  in order to separate the decay rate into two  $\mu$ -independent pieces, as displayed in Eq. (3). For power counting purposes,  $\mu_0 \sim \mu_b \sim m_b$  and formally  $\mu_0 \geq \mu_b$ . For numerical work one can take  $\mu_0 = \mu_b$ .

In Eq. (13) we begin with a complete set of Dirac structures for the vector and tensor currents in SCET, namely

$$\Gamma_{a-c}^{(v)} = P_R \left\{ \gamma^\mu, v^\mu, \frac{n^\mu}{n \cdot v} \right\}, \quad \Gamma_{a-d}^{(t)} = P_R \frac{q_\tau}{q^2} \left\{ i\sigma^{\mu\tau}, \gamma^{[\mu} v^{\tau]}, \frac{\gamma^{[\mu} n^{\tau]}}{n \cdot v}, \frac{n^{[\mu} v^{\tau]}}{n \cdot v} \right\}. \quad (18)$$

These come with Wilson coefficients  $C_{9a,b,c}$  and  $C_{7a,b,c,d}$  respectively. This basis is over-complete for  $B \rightarrow X_s \ell^+ \ell^-$ , but considering a redundant basis makes it easy to incorporate pre-existing perturbative calculations for the currents into our computations. Only the coefficients  $C_{7a,9a}$  appear at tree level, but for heavy-to-light currents it is known that the other structures become relevant once perturbative corrections are included. For simplicity of notation, we treat the  $1/q^2$  photon propagator in  $\Gamma_j^{(t)}$  as part of the effective-theory operator.<sup>2</sup>

To further reduce the basis in Eq. (18) we can use i) current conservation,  $q^\mu \bar{\ell} \gamma_\mu \ell = 0$ , ii)  $q^\mu \bar{\ell} \gamma_\mu \gamma_5 \ell = 0$  for massless leptons, iii) a reduction of the tensor  $\Gamma^{(t)}$  Dirac structures into vector structures, since they are all contracted with  $q_\tau$ . Constraint ii) allows us to eliminate  $C_{10c}$ . Taken together, constraints i) and iii) allow us to reduce the seven terms  $C_{9i}$  and  $C_{7i}$  to two independent coefficients. For our new basis of operators we take

$$\begin{aligned} J_{\ell\ell}^{(0)} &= \mathcal{C}_9 (\bar{\chi}_{n,p} P_R \gamma^\mu \mathcal{H}_v) (\bar{\ell} \gamma_\mu \ell) - \mathcal{C}_7 \frac{2m_B q_\tau}{q^2} (\bar{\chi}_{n,p} P_R i\sigma^{\mu\tau} \mathcal{H}_v) (\bar{\ell} \gamma_\mu \ell) \\ &\quad + \mathcal{C}_{10a} (\bar{\chi}_{n,p} P_R \gamma^\mu \mathcal{H}_v) (\bar{\ell} \gamma_\mu \gamma_5 \ell) + \mathcal{C}_{10b} (\bar{\chi}_{n,p} P_R v^\mu \mathcal{H}_v) (\bar{\ell} \gamma_\mu \gamma_5 \ell), \end{aligned} \quad (19)$$

and find that

$$\begin{aligned} \mathcal{C}_9 &= C_{9a} + \frac{C_{9b}}{2} - \frac{m_B}{n \cdot q} C_{7b} + \frac{2m_B(C_{7c} - C_{7d}) + n \cdot q C_{9c}}{n \cdot q - \bar{n} \cdot q}, \\ \mathcal{C}_7 &= C_{7a} - \frac{C_{7b}}{2} - \frac{\bar{n} \cdot q}{4m_B} C_{9b} + \frac{1}{n \cdot q - \bar{n} \cdot q} \left[ \frac{-q^2}{2m_B} C_{9c} - n \cdot q C_{7c} + \bar{n} \cdot q C_{7d} \right], \\ \mathcal{C}_{10a} &= C_{10a}, \\ \mathcal{C}_{10b} &= C_{10b} + \frac{2n \cdot q}{n \cdot q - \bar{n} \cdot q} C_{10c}. \end{aligned} \quad (20)$$

Our Dirac structures for the  $\mathcal{C}_9$  and  $\mathcal{C}_7$  terms in Eq. (19) were deliberately chosen, in order to make results for the decay rates appear as much as possible like those in the local OPE. The fact that the basis of SCET operators for  $B \rightarrow X_s \ell^+ \ell^-$  involves only bilinear hadronic currents at LO means that in the leading-order factorization theorem we find the exact

<sup>2</sup> If we instead demand that the momentum  $q^2$  be collinear in the  $\bar{n}$  direction, with  $s \sim \lambda^2$ , then the SCET operator with a photon field strength should be kept, and will then be contracted with an operator with collinear leptons within SCET. In this case there will also be additional four-quark operators needed in the basis in Eq. (19).

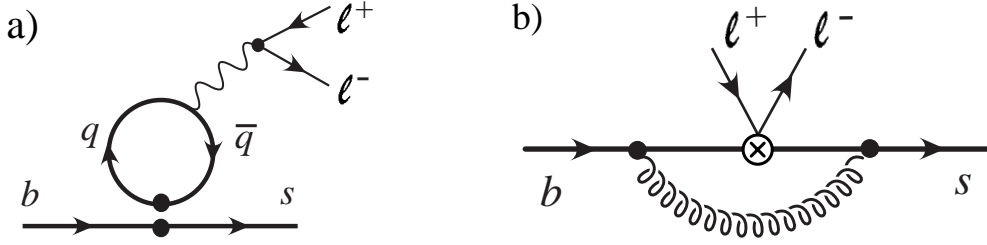


FIG. 2: Graphs from  $H_W$  for matching on to SCET.

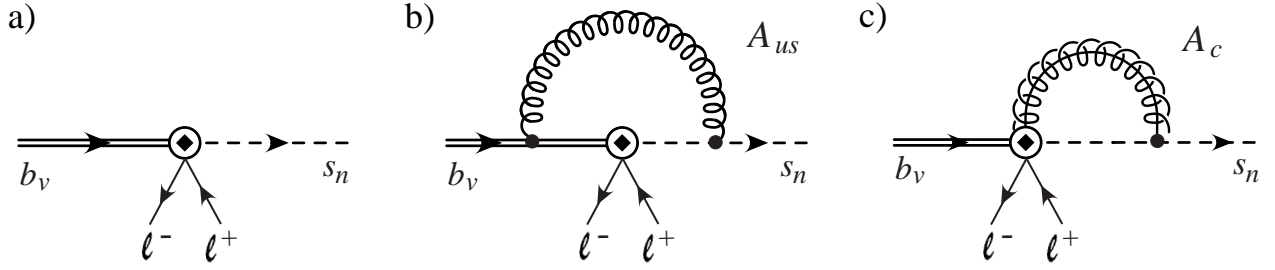


FIG. 3: Graphs in SCET for the matching computation.

same non-perturbative shape function as for  $B \rightarrow X_s \gamma$  and  $B \rightarrow X_u \ell \bar{\nu}$ . This is immediately evident from the operator-based proof of factorization in Ref. [28], for example. While the coefficients  $C_{9i}$ ,  $C_{7i}$ ,  $C_{10i}$  in Eq. (13) are functions only of  $s = (n \cdot q)(\bar{n} \cdot q)/m_b^2$ , the reduction of the basis of operators brings in additional kinematic dependence on  $\bar{n} \cdot q$  and  $n \cdot q$  for the  $C_i$ 's (which is also the case in analyzing exclusive dilepton decays [47]). At tree level we have  $\mathcal{O}_{9,10}$  contributing to  $C_{9a}$  and  $C_{10a}$ , and a contribution from  $\mathcal{O}_7$  with the photon producing an  $\ell^+ \ell^-$  pair, which give

$$\mathcal{C}_9 = C_9^{\text{NDR}}(\mu_0), \quad \mathcal{C}_7 = \frac{\bar{m}_b(\mu_0)}{m_B} C_7^{\text{NDR}}(\mu_0), \quad \mathcal{C}_{10a} = C_{10}, \quad \mathcal{C}_{10b} = 0. \quad (21)$$

Beyond tree level there will be  $C_7$  dependence in  $\mathcal{C}_9$ , and  $C_9$  dependence in  $\mathcal{C}_7$ . Eq. (21) indicates that with our choice of basis the same short distance dependence dominates in SCET,  $\mathcal{C}_9 \approx C_9$ , etc. We explore this further in Section III E. In Eq. (21) there is no distinction as to whether this matching is done at  $\mu = \mu_0$  or  $\mu = \mu_b$ . The effective-theory operator in Eq. (19) was defined with a factor of  $m_B$  pulled out so that the  $\mu$ -dependent factors  $\bar{m}_b C_7^{\text{NDR}}$  are contained in the coefficients  $\mathcal{C}_7$ .

At one-loop order, the full-theory diagrams needed for the matching are shown in Fig. 2 (plus wavefunction renormalization, which is not shown). At this order the four-quark operators  $\mathcal{O}_{1-6}$  contribute through Fig. 2a. The one-loop graphs in SCET with the operators in Eq. (19) are shown in Fig. 3 (plus wavefunction renormalization, which is not shown). There are no graphs with four-quark operators within SCET since we treat  $q^2 \sim \lambda^0$ , so Fig. 2a matches directly on to  $\mathcal{C}_9$ .

As discussed in the introduction, we perform a split-matching procedure from the full theory above  $m_b$  on to SCET below  $m_b$ , making use of two matching scales  $\mu_0$  and  $\mu_b$ .

Contributions from this stage of matching therefore take the form

$$\mathcal{B}(\mu_0, \mu_b) = B_1(\mu_0)B_2(\mu_b). \quad (22)$$

Since  $\mathcal{O}_{10}$  has no anomalous dimension above  $m_b$  and there is a common universal anomalous dimension for all the operators in  $J_{\ell\ell}^{(0)}$  below  $m_b$ , there is a well-defined prescription for carrying this out. We take all contributions that cause perturbative corrections to  $\mathcal{C}_{10a}$  and  $\mathcal{C}_{10b}$  to be at the scale  $\mu_b$ , so for this operator  $B_1(\mu_0) = C_{10}$ , and at one-loop order  $B_2(\mu_b)$  includes  $\alpha_s(\mu_b) \ln^2(\mu_b)$ ,  $\alpha_s(\mu_b) \ln(\mu_b)$ , and  $\alpha_s(\mu_b)$  terms from matching the vertex diagram Fig. 2b and wavefunction diagrams on to SCET. The analogous contributions from vertex diagrams for  $\mathcal{C}_9$  and  $\mathcal{C}_7$  are also matched at  $\mu = \mu_b$  to determine their  $B_2(\mu_b)$ 's (for  $\mathcal{C}_7$  the full-theory tensor current has a  $\ln \mu$  that is matched at  $\mu = \mu_0$ ). The universality of the anomalous dimensions in SCET guarantees that this procedure remains well defined at any order in perturbation theory and can be organized into the product structure displayed in Eq. (22). For  $\mathcal{C}_9$  and  $\mathcal{C}_7$  there are additional non-vertex-like contributions that are matched on to  $B_1(\mu_0)$  at a scale  $\mu_0 \geq \mu_b$ . These include contributions from four-quark operators  $\mathcal{O}_{1-6}$  in the full theory, which will match on to  $\mathcal{C}_9$  and  $\mathcal{C}_7$  in SCET.

The difference between the full-theory diagram in Fig. 2b and the SCET graphs in Fig. 3b,c is IR finite (where we must use the same IR regulator in both theories, as is always the case for matching computations). In the UV the full-theory graph in Fig. 2b plus wavefunction renormalization is  $\mu$ -independent since the current is conserved. The graphs in SCET induce a  $\mu$  dependence and an anomalous dimension for the effective-theory currents. These terms are matched at  $\mu = \mu_b$ . We start with the basis in Eq. (13) and find

$$\begin{aligned} C_{10a}(\mu_0, \mu_b) &= C_{10} \left[ 1 + \frac{\alpha_s(\mu_b)}{\pi} \omega_a^V(s, \mu_b) \right], \\ C_{10b,10c}(\mu_0, \mu_b) &= C_{10} \frac{\alpha_s(\mu_b)}{\pi} \omega_{b,c}^V(s), \end{aligned} \quad (23)$$

with a constant  $\mu_0$ -independent  $C_{10}$ . The perturbative coefficients were computed in Ref. [26], and setting  $\bar{n} \cdot p/m_b = (1-s)$  we find

$$\begin{aligned} \omega_a^V(s, \mu_b) &= -\frac{1}{3} \left[ 2\ln^2(1-s) + 2\text{Li}_2(s) + \ln(1-s) \left( \frac{1-3s}{s} \right) + \frac{\pi^2}{12} + 6 \right. \\ &\quad \left. + 2\ln^2\left(\frac{\mu_b}{m_b}\right) + 5\ln\left(\frac{\mu_b}{m_b}\right) - 4\ln(1-s)\ln\left(\frac{\mu_b}{m_b}\right) \right], \\ \omega_b^V(s) &= \frac{1}{3} \left[ \frac{2}{s} + \frac{2(1-s)}{s^2} \ln(1-s) \right], \\ \omega_c^V(s) &= \frac{1}{3} \left[ \frac{(2s-1)(1-s)}{s^2} \ln(1-s) - \frac{(1-s)}{s} \right]. \end{aligned} \quad (24)$$

For the matching on to  $C_{9a,b,c}$  in the basis in Eq. (13) we have the same perturbative coefficients  $\omega_{a,b,c}$  as for  $C_{10a,b,c}$ , because only the leptonic current differs:

$$\begin{aligned} C_{9a}(\mu_0, \mu_b) &= C_9^{\text{mix}}(\mu_0) \left[ 1 + \frac{\alpha_s(\mu_b)}{\pi} \omega_a^V(s, \mu_b) \right], \\ C_{9b,9c}(\mu_0, \mu_b) &= C_9^{\text{mix}}(\mu_0) \left[ \frac{\alpha_s(\mu_b)}{\pi} \omega_{b,c}^V(s) \right]. \end{aligned} \quad (25)$$

However, for  $C_{9i}$  there are additional contributions,  $C_9^{\text{mix}}(\mu_0)$ , from the matching at  $\mu = \mu_0$ , which at one-loop order and  $\mathcal{O}(\alpha_s^0)$  includes Fig. 2a:

$$\begin{aligned} C_9^{\text{mix}}(\mu_0) &= C_9^{\text{NDR}}(\mu_0) + \frac{2}{9} (3C_3 + C_4 + 3C_5 + C_6) - \frac{1}{2} h(1, s) (4C_3 + 4C_4 + 3C_5 + C_6) \\ &\quad + h\left(\frac{m_c}{m_b}, s\right) (3C_1 + C_2 + 3C_3 + C_4 + 3C_5 + C_6) - \frac{1}{2} h(0, s) (C_3 + 3C_4) \\ &\quad + \frac{\alpha_s(\mu_0)}{\pi} C_9^{\text{mix}(1)}(\mu_0), \end{aligned} \quad (26)$$

where all running coefficients on the RHS are  $C_i = C_i(\mu_0)$ . We shall discuss the relation of  $C_9^{\text{mix}}$  to  $\tilde{C}_9^{\text{eff}}$  in in the local OPE analysis [9, 10] after Eq.(33). In Eq. (26) the functions  $h(1, s)$ ,  $h(z, s)$ , and  $h(0, s)$  for the b-quark, c-quark, and light-quark penguin loops are [8, 10]

$$\begin{aligned} h(z, s) &= \frac{8}{9} \ln\left(\frac{\mu_0}{m_b}\right) - \frac{8}{9} \ln z + \frac{8}{27} + \frac{4}{9} \zeta - \frac{2}{9} (2 + \zeta) \sqrt{|1 - \zeta|} \\ &\quad \times \left[ \theta(1 - \zeta) \left( -i\pi + \ln \frac{1 + \sqrt{1 - \zeta}}{1 - \sqrt{1 - \zeta}} \right) + \theta(\zeta - 1) 2 \arctan \frac{1}{\sqrt{\zeta - 1}} \right], \\ h(0, s) &= \frac{8}{27} + \frac{8}{9} \ln\left(\frac{\mu_0}{m_b}\right) - \frac{4}{9} \ln s + \frac{4}{9} i\pi, \end{aligned} \quad (27)$$

with  $\zeta = 4z^2/s$ . Higher-order  $\mathcal{O}(\alpha_s)$  corrections in Eq. (26) are denoted by the  $C_9^{\text{mix}(1)}$  term. An important class of these corrections from mixing can be determined from the NNLL analysis in Refs. [12, 13, 15]:

$$C_9^{\text{mix}(1)}(\mu_0) = C_8^{\text{NDR}} \kappa_{8 \rightarrow 9}(s, \mu_0) + C_1 \kappa_{1 \rightarrow 9}(s, \mu_0, \hat{m}_c) + C_2 \kappa_{2 \rightarrow 9}(s, \mu_0, \hat{m}_c). \quad (28)$$

To determine these terms one must be careful to separate out the factors in square brackets in Eq. (25). However we shall not attempt to include all NNLL terms consistently here. Contributions to  $C_9^{\text{mix}(1)}$  from the penguin coefficients  $C_{3-6}$  are unknown but expected to be small (at the  $\sim 1\%$  level).

Lastly, we turn to the results for  $C_{7i}$ . From the vertex graphs we have

$$\begin{aligned} C_{7a}(\mu_0, \mu_b) &= C_7^{\text{mix}}(\mu_0) \left[ 1 + \frac{\alpha_s(\mu_b)}{\pi} \omega_a^T(s, \mu_b) \right], \\ C_{7b,7c,7d}(\mu_0, \mu_b) &= C_7^{\text{mix}}(\mu_0) \frac{\alpha_s(\mu_b)}{\pi} \omega_{b,c,d}^T(s). \end{aligned} \quad (29)$$

The  $\omega_i^T$  perturbative corrections are again determined from the SCET matching in Ref. [26], which (switching to  $s$ ) gives

$$\begin{aligned} \omega_a^T(s, \mu_b) &= -\frac{1}{3} \left[ 2\ln^2(1-s) + 2\text{Li}_2(s) + \ln(1-s) \left( \frac{2-4s}{s} \right) + \frac{\pi^2}{12} + 6 \right. \\ &\quad \left. + 2\ln^2\left(\frac{\mu_b}{m_b}\right) + 5\ln\left(\frac{\mu_b}{m_b}\right) - 4\ln(1-s)\ln\left(\frac{\mu_b}{m_b}\right) \right], \\ \omega_b^T(s) &= \omega_d^T(s) = 0, \\ \omega_c^T(s) &= \frac{1}{3} \left[ \frac{-2(1-s)\ln(1-s)}{s} \right]. \end{aligned} \quad (30)$$

Additional contributions from other diagrams are matched at the scale  $\mu_0$  into  $C_7^{\text{mix}}(\mu_0)$ . Note that, unlike the vector currents, the tensor current for  $O_7$  gets renormalized for  $\mu > m_b$  and we must include the corresponding  $\ln(\mu_0/m_b)$  in  $C_7^{\text{mix}}(\mu_0)$ , i.e.

$$C_7^{\text{mix}}(\mu_0) = \frac{\bar{m}_b(\mu_0)}{m_B} \left\{ C_7^{\text{NDR}}(\mu_0) \left[ 1 - \frac{2\alpha_s(\mu_0)}{3\pi} \ln\left(\frac{\mu_0}{m_b}\right) \right] + \frac{\alpha_s(\mu_0)}{\pi} C_7^{\text{mix}(1)}(\mu_0) \right\}, \quad (31)$$

where, much like in the case of  $C_9^{\text{mix}}$ , we have

$$C_7^{\text{mix}(1)}(\mu_0) = C_8^{\text{NDR}} \kappa_a^8(s, \mu_0) + C_1 \kappa_a^1(s, \mu_0, \hat{m}_c) + C_2 \kappa_a^2(s, \mu_0, \hat{m}_c), \quad (32)$$

and the results for  $\kappa_{8 \rightarrow 7}(s, \mu_0)$ ,  $\kappa_{1 \rightarrow 7}(s, \mu_0, \hat{m}_c)$ , and  $\kappa_{2 \rightarrow 7}(s, \mu_0, \hat{m}_c)$  can be found in Ref. [48]. Contributions to  $C_7^{\text{mix}(1)}$  from the penguin coefficients  $C_{3-6}$  can be found in Ref. [49].

Using Eq. (20),  $\bar{n} \cdot q n \cdot q / m_B^2 = y_H$ , and  $n \cdot q / m_B = 1 - u_H$ , we can use the above results to give the final coefficients for our basis of operators with the minimal number of Dirac structures, namely

$$\begin{aligned} \mathcal{C}_9 &= C_9^{\text{mix}}(\mu_0) \left\{ 1 + \frac{\alpha_s(\mu_b)}{\pi} \left[ \omega_a^V(s, \mu_b) + \frac{1}{2} \omega_b^V(s) + \frac{(1-u_H)^2 \omega_c^V(s)}{(1-u_H)^2 - y_H} \right] \right\} \\ &\quad + C_7^{\text{mix}}(\mu_0) \frac{\alpha_s(\mu_b)}{\pi} \left[ \frac{2(1-u_H)[\omega_c^T(s) - \omega_d^T(s)]}{(1-u_H)^2 - y_H} - \frac{\omega_b^T(s)}{(1-u_H)} \right], \\ \mathcal{C}_7 &= C_7^{\text{mix}}(\mu_0) \left\{ 1 + \frac{\alpha_s(\mu_b)}{\pi} \left[ \omega_a^T(s, \mu_b) - \frac{1}{2} \omega_b^T(s) + \frac{y_H \omega_d^T(s) - (1-u_H)^2 \omega_c^T(s)}{(1-u_H)^2 - y_H} \right] \right\} \\ &\quad - C_9^{\text{mix}}(\mu_0) \frac{\alpha_s(\mu_b)}{\pi} \left[ \frac{y_H \omega_b^V(s)}{4(1-u_H)} + \frac{y_H (1-u_H) \omega_c^V(s)}{2[(1-u_H)^2 - y_H]} \right], \\ \mathcal{C}_{10a} &= C_{10} \left\{ 1 + \frac{\alpha_s(\mu_b)}{\pi} \omega_a^V(s, \mu_b) \right\}, \\ \mathcal{C}_{10b} &= C_{10} \frac{\alpha_s(\mu_b)}{\pi} \left[ \omega_b^V(s) + \frac{2(1-u_H)^2}{(1-u_H)^2 - y_H} \omega_c^V(s) \right], \end{aligned} \quad (33)$$

where the terms have the structure of a sum over products  $B_1(\mu_0)B_2(\mu_b)$ , as desired.

In using the results in Eq. (33) one can choose to work to different orders in the  $\mu_0$ - and  $\mu_b$ -dependent terms, as shown in Eq. (3). For the  $\mu_0$  dependence,  $C_9^{\text{mix}}(\mu_0)$  and  $C_7^{\text{mix}}(\mu_0)$  include terms from matching at  $m_W$  and running to  $m_b$ , as well as matching contributions at  $m_b$  that cancel the  $\mu_0$  dependence from the other pieces. Thus, these coefficients have only a small residual  $\mu_0$  dependence, which is canceled at higher orders, just as in the local OPE. The  $\mathcal{C}_i$  coefficients depend on  $\mu_b$ , both through  $\alpha_s(\mu_b)$  and through explicit  $\mu_b$  dependence in  $\omega_a^T$  and  $\omega_a^V$ . The  $\ln \mu_b$  dependence in  $\omega_a^V$  and  $\omega_a^T$  is identical, as expected from the known independence of the anomalous dimension on the Dirac structure in SCET. The  $\mu_b$  dependence in  $\mathcal{C}_i(\mu_b, \mu_0)$  is universal, and will cancel against the universal  $\mu_b$  dependence in the jet and shape functions, which they multiply in the decay rates. We consider the phenomenological organization of the perturbative series for  $\mu_0$  and  $\mu_b$  terms in turn.

First consider the  $\mu_0$  terms. Because of mixing, the sizes of contributions to  $C_9^{\text{NDR}}$  are comparable at LL and NLL orders [9, 10], so a reasonable first approximation is to take

the NLL result (just as for the local OPE decay rate). This entails dropping the  $\mathcal{O}(\alpha_s)$  matching corrections  $C_9^{\text{mix}(1)}$  and  $C_7^{\text{mix}(1)}$ , and running  $C_9$  at NLL order with  $C_7$  at LL order. As an improved approximation, we would then adopt the operationally well-defined NNLL approach [12] of running both  $C_9$  and  $C_7$  to NLL order and keeping the  $\mathcal{O}(\alpha_s)$  matching corrections at  $m_b$ .<sup>3</sup>

Below  $m_b$  there are Sudakov logarithms. For the  $\mu_b$  dependence, the RG evolution in SCET sums these double-logarithmic series. As a first approximation we could take the LL and NLL running in  $U_H(\mu_b, \mu_i)$  and  $U_S(\mu_i, \mu_\Lambda)$  in Eq. (3), while using tree-level matching for  $B_2(\mu_b)$  and  $\mathcal{J}(\mu_i)$ . This is consistent because the NLL running is equivalent to LL running in a single-log resummation. As a second approximation we could then take NNLL running in both terms and include one-loop matching for both  $B_2(\mu_b)$  and  $\mathcal{J}(\mu_i)$ . However since the scales  $m_b^2 \gg m_b \Lambda \gg 1 \text{ GeV}^2$  are not as well separated as  $m_W^2 \gg m_b^2$ , we could instead consider the second approximation to include the one-loop matching for  $B_2(\mu_b)$  and  $\mathcal{J}(\mu_i)$  with NLL running, but without including the full NNLL running (for which parts remain unknown).

Our procedure for split matching above was based on the non-renormalization of  $\mathcal{O}_{10}$  in QCD. It can also be thought of as matching in two steps. First one matches at  $\mu_0$  on to the scale-invariant operators

$$\begin{aligned}
J^{(0)} &= C_9^{\text{mix}} (\bar{s} P_R \gamma^\mu b) (\bar{\ell} \gamma_\mu \ell) + C_{10} (\bar{s} P_R \gamma^\mu b) (\bar{\ell} \gamma_\mu \gamma_5 \ell) \\
&\quad - C_7^{\text{mix}} \frac{2m_B q_\tau}{q^2} [(\bar{s} P_R i \sigma^{\mu\tau} b)(\mu = m_b)] (\bar{\ell} \gamma_\mu \ell),
\end{aligned} \tag{34}$$

to determine the coefficients  $C_{7,9}^{\text{mix}}$ . These coefficients are  $\mu_0$  independent at the order in perturbation theory to which the matching is done. Secondly, the operators in Eq. (34) are matched on to the SCET currents in Eq. (19) at the scale  $\mu_b$  to determine the coefficients  $\mathcal{C}_7, \mathcal{C}_9, \mathcal{C}_{10a,b}$ . In Eq. (34) the operators for  $C_9^{\text{mix}}$  and  $C_{10}$  are conserved, but the tensor current has an anomalous dimension, and so we take  $\mu = m_b$  as a reference point for matching on to a scale-invariant operator. This choice corresponds to the  $\ln m_b$  factor in Eq. (31) for  $C_7^{\text{mix}}$ . A different choice will affect the division of  $\alpha_s(\mu_0)$  or  $\alpha_s(\mu_b)$  terms. Note that Eq. (34) should be thought of only as an auxiliary step to facilitate the split matching; there is no sense in which the running of the tensor current is relevant by itself. In general the split-matching procedure could be carried out in a manner that gives different constant terms at a given order, but any such ambiguity will cancel order by order in  $\mathcal{C}_7$  and  $\mathcal{C}_9$  (and explicitly if  $\mu_0 = \mu_b$ ).

Finally, note that our  $\omega_a$  differs from the result for  $\omega^{\text{OPE}}$  identified in Ref. [10] for the partonic semileptonic decay rate when using the local OPE,

$$\begin{aligned}
\omega_{\text{semi}}^{\text{OPE}} &= -\frac{1}{3} \left[ 2\ln(s) \ln(1-s) + 4\text{Li}_2(s) + \ln(1-s) \left( \frac{5+4s}{1+2s} \right) + \frac{2s(1+s)(1-2s)}{(1-s)^2(1+2s)} \ln(s) \right. \\
&\quad \left. - \frac{(5+9s-6s^2)}{2(1-s)(1+2s)} + \frac{2\pi^2}{3} \right].
\end{aligned} \tag{35}$$

Here  $\omega_{\text{semi}}^{\text{OPE}}$  contains both vertex and bremsstrahlung contributions evaluated in the full theory. At LO, the restricted phase space in the shape function region causes bremsstrahlung

---

<sup>3</sup> We assume that matching at the high scale,  $m_W$ , is always done at the order appropriate to the running of  $U_W(\mu_W, \mu_0)$  in Eq. (3).

to contribute only to the jet and shape functions, and not at the scale  $\mu \simeq m_b$ . The shape function and jet function also modify the contributions from the vertex graphs. Thus, instead of  $\omega_{semi}^{OPE}$  the final results in the shape function region are given by our  $\omega_i^V$  and  $\omega_i^T$  factors. Consequently, the main difference is in the terms we match at  $\mu = \mu_b$ , while the terms matched at  $\mu = \mu_0$  that appear in  $C_9^{\text{mix}}$  and  $C_7^{\text{mix}}$  are identical to terms appearing in the local OPE analysis.

## B. RG Evolution Between $\mu_b$ and $\mu_i$

The running of the Wilson coefficients in SCET from the scale  $\mu_b^2 \sim m_b^2$  to  $\mu_i^2 \sim m_b \Lambda_{\text{QCD}}$  involves double Sudakov logarithms and was derived in Refs. [25, 26] at NLL order. The SCET running is independent of the Dirac structure of the currents, and all coefficients obey the same homogeneous anomalous dimension equation,

$$\begin{aligned} \mu \frac{d}{d\mu} \mathcal{C}_i(\mu) &= \left[ -\Gamma_{\text{cusp}}(\alpha_s) \ln\left(\frac{\mu}{\bar{\mathcal{P}}}\right) + \tilde{\gamma}(\alpha_s) \right] \mathcal{C}_i(\mu) \\ &= \left[ -\Gamma_{\text{cusp}}(\alpha_s) \ln\left(\frac{\mu}{\mu_b}\right) + \left\{ \tilde{\gamma}(\alpha_s) + \Gamma_{\text{cusp}}(\alpha_s) \ln\left(\frac{\bar{n}\cdot p}{\mu_b}\right) \right\} \right] \mathcal{C}_i(\mu). \end{aligned} \quad (36)$$

This must be integrated together with the beta function  $\beta = \mu d/d\mu \alpha_s(\mu)$  to solve for  $U_H$  in

$$\mathcal{C}_i(\mu_i) = \sqrt{U_H(\mu_i, \mu_b)} \mathcal{C}_i(\mu_b). \quad (37)$$

In the second line of Eq. (36) we used the fact that  $\bar{\mathcal{P}}$  gives the total partonic  $\bar{n}\cdot p$  momentum of the jet  $X_s$  in the  $B \rightarrow X_s \ell^+ \ell^-$  matrix element, and we introduced artificial dependence on the matching scale  $\mu_b$  in order to make the  $\bar{n}\cdot p$  dependence appear in a small logarithm. Here  $\bar{n}\cdot p = m_b - \bar{n}\cdot q$ . We write

$$\Gamma^{\text{cusp}} = \sum_{n=0}^{\infty} \Gamma_n^{\text{cusp}} \left(\frac{\alpha_s}{4\pi}\right)^{n+1}, \quad \tilde{\gamma} = \sum_{n=0}^{\infty} \tilde{\gamma}_n \left(\frac{\alpha_s}{4\pi}\right)^{n+1}, \quad \beta = -2\alpha_s \sum_{n=0}^{\infty} \beta_n \left(\frac{\alpha_s}{4\pi}\right)^{n+1}. \quad (38)$$

At NLL order we need  $\beta_0 = 11C_A/3 - 2n_f/3$ ,  $\beta_1 = 34C_A^2/3 - 10C_A n_f/3 - 2C_F n_f$  and

$$\Gamma_0^{\text{cusp}} = 4C_F, \quad \Gamma_1^{\text{cusp}} = 8C_F B = 8C_F \left[ C_A \left( \frac{67}{18} - \frac{\pi^2}{6} \right) - \frac{5}{9} n_f \right], \quad \tilde{\gamma}_0 = -5C_F, \quad (39)$$

where  $C_A = 3$  and  $C_F = 4/3$  for SU(3). For the number of active flavors we take  $n_f = 4$  since we're running below  $m_b$ . The cusp anomalous dimension  $\Gamma_1^{\text{cusp}}$  was computed in Ref. [50], and the result for  $\Gamma_2^{\text{cusp}}$  was recently found in Ref. [51]. RG evolution in SCET at NNLL order has been considered in Refs. [43, 52]. For the NNLL result one needs  $\Gamma_2^{\text{cusp}}$ ,  $\tilde{\gamma}_1$ , and  $\beta_2$ . For  $\tilde{\gamma}_1$  an independent calculation does not exist, but a conjecture for its value was given in Ref. [43] based on the structure of the three loop splitting function [51]. For the sake of clarity we stick to NLL order here. The result is

$$U_H(\mu_i, \mu_b) = \exp \left[ \frac{2g_0(r_1)}{\alpha_s(\mu_b)} + 2g_1(r_1, \bar{n}\cdot p) \right], \quad (40)$$

where the independent variable is  $\mu_i$  and

$$r_1(\mu_i) = \frac{\alpha_s(\mu_i)}{\alpha_s(\mu_b)} = \frac{2\pi}{2\pi + \beta_0 \alpha_s(\mu_b) \ln(\mu_i/\mu_b)}, \quad (41)$$

with

$$\begin{aligned} g_0(r_1) &= -\frac{4\pi C_F}{\beta_0^2} \left[ \frac{1}{r_1} - 1 + \ln r_1 \right], \\ g_1(r_1, \bar{n} \cdot p) &= -\frac{C_F \beta_1}{\beta_0^3} \left[ 1 - r_1 + r_1 \ln r_1 - \frac{1}{2} \ln^2 r_1 \right] \\ &\quad + \frac{C_F}{\beta_0} \left[ \frac{5}{2} - 2 \ln \left( \frac{\bar{n} \cdot p}{\mu_b} \right) \right] \ln r_1 - \frac{2C_F B}{\beta_0^2} \left[ r_1 - 1 - \ln r_1 \right]. \end{aligned} \quad (42)$$

This is the form for the universal running of the LO SCET currents found in Ref. [26]. Switching to  $\alpha_s(\mu_i)$  as the independent variable, with  $r_1 = \alpha_s(\mu_i)/\alpha_s(\mu_b)$ , gives

$$U_H(\mu_i, \mu_b) = \left( \frac{\bar{n} \cdot p}{\mu_b} \right)^{-\frac{4C_F}{\beta_0} \ln r_1} \exp \left[ \frac{2g_0(r_1)}{\alpha_s(\mu_b)} + 2\tilde{g}_1(r_1) \right], \quad (43)$$

where  $g_0(r_1)$  is as in Eq. (42) and

$$\tilde{g}_1(r_1) = \frac{C_F \beta_1}{2\beta_0^3} \ln^2 r_1 + \frac{5C_F}{2\beta_0} \ln r_1 + \frac{C_F}{\beta_0^3} (2B\beta_0 - \beta_1) (1 - r_1 + \ln r_1). \quad (44)$$

This form of the evolution with  $\alpha_s(\mu)$  as the variable was used in Ref. [33], and is also the one we adopt here. The decay rate is computed from a time-ordered product of currents and so at the intermediate scale  $\mu_i^2 \sim m_b \Lambda$  will involve products

$$\mathcal{C}_i(\mu_i, \mu_0) \mathcal{C}_j(\mu_i, \mu_0) = U_H(\mu_i, \mu_b) \mathcal{C}_i(\mu_b, \mu_0) \mathcal{C}_j(\mu_b, \mu_0), \quad (45)$$

explaining why we used a notation with  $\sqrt{U_H}$  in Eq. (37).

### C. Hadronic Tensor and Decay Rates

In the last two sections we constructed the required basis of SCET current operators with matching at  $\mu_0^2 \sim \mu_b^2 \sim m_b^2$  and evolution to  $\mu_i^2 \sim m_b \Lambda$ . At the scale  $\mu_i$  we take time-ordered products of the SCET currents and compute the decay rates using the optical theorem. In this section we discuss the tensor decomposition of the time-ordered products and results for differential decay rates.

In order to simplify the computation of decay rates it is useful to write the sum of hadronic operators as a sum of left-handed and right-handed terms since for massless leptons we have only LL or RR contributions [19]. Doing this for our current, we have

$$\begin{aligned} \mathcal{J}_{\ell\ell}^{(0)} &= [\mathcal{C}_9 - \mathcal{C}_{10a}] (\bar{\chi}_n \gamma_\mu P_L \mathcal{H}_v) (\bar{\ell} \gamma^\mu P_L \ell) + [\mathcal{C}_9 + \mathcal{C}_{10a}] (\bar{\chi}_n \gamma_\mu P_L \mathcal{H}_v) (\bar{\ell} \gamma^\mu P_R \ell) \\ &\quad + \mathcal{C}_{10b} (\bar{\chi}_n v_\mu P_R \mathcal{H}_v) (\bar{\ell} \gamma^\mu \gamma_5 \ell) - \mathcal{C}_7 \frac{2m_B q^\tau}{q^2} (\bar{\chi}_n i\sigma_{\mu\tau} \mathcal{H}_v) (\bar{\ell} \gamma^\mu l) \\ &= (J_{L\mu} L_L^\mu + J_{R\mu} L_R^\mu), \end{aligned} \quad (46)$$

where

$$\begin{aligned}
L_L^\mu &= \bar{\ell} \gamma^\mu P_L \ell, & L_R^\mu &= \bar{\ell} \gamma^\mu P_R \ell, \\
J_{L(R)}^\mu &= \bar{\chi}_n P_R \left[ (\mathcal{C}_9 \mp \mathcal{C}_{10a}) \gamma^\mu + \mathcal{C}_7 \frac{2m_B \gamma^\mu \not{q}}{q^2} \mp \mathcal{C}_{10b} v^\mu \right] \mathcal{H}_v \\
&\equiv \bar{\chi}_n \Gamma_{L(R)}^\mu \mathcal{H}_v.
\end{aligned} \tag{47}$$

Thus, the inclusive decay rate for  $\bar{B} \rightarrow X_s \ell^+ \ell^-$  is proportional to  $(W_{\mu\nu}^L L_L^{\mu\nu} + W_{\mu\nu}^R L_R^{\mu\nu})$ , where the leptonic parts  $L_{L(R)}^{\mu\nu}$  and hadronic parts  $W_{L(R)}^{\mu\nu}$  are given by

$$\begin{aligned}
L_{L(R)}^{\mu\nu} &= \sum_{\text{spin}} [\bar{l}_{L(R)}(p_+) \gamma^\mu l_{L(R)}(p_-)] [\bar{l}_{L(R)}(p_-) \gamma^\nu l_{L(R)}(p_+)] \\
&= 2 [p_+^\mu p_-^\nu + p_-^\mu p_+^\nu - g^{\mu\nu} p_+ \cdot p_- \mp i \epsilon^{\mu\nu\alpha\beta} p_{+\alpha} p_{-\beta}],
\end{aligned} \tag{48}$$

and

$$\begin{aligned}
W_{\mu\nu}^{L(R)} &= \frac{1}{2m_B} \sum_X (2\pi)^3 \delta^4(p_B - q - p_X) \langle \bar{B} | J_\mu^{L(R)\dagger} | X \rangle \langle X | J_\nu^{L(R)} | \bar{B} \rangle \\
&= -g_{\mu\nu} W_1^{L(R)} + v_\mu v_\nu W_2^{L(R)} + i \epsilon_{\mu\nu\alpha\beta} v^\alpha q^\beta W_3^{L(R)} + q_\mu q_\nu W_4^{L(R)} + (v_\mu q_\nu + v_\nu q_\mu) W_5^{L(R)}.
\end{aligned} \tag{49}$$

Here, we use relativistic normalization for the  $|\bar{B}\rangle$  states. For convenience, we define projection tensors  $P_i^{\mu\nu}$  so that

$$W_i^{L(R)} = P_i^{\mu\nu} W_{\mu\nu}^{L(R)}. \tag{50}$$

They are

$$\begin{aligned}
P_1^{\mu\nu} &= -\frac{1}{2} g^{\mu\nu} + \frac{q^2 v^\mu v^\nu + q^\mu q^\nu - v \cdot q (v^\mu q^\nu + v^\nu q^\mu)}{2[q^2 - (v \cdot q)^2]}, \\
P_2^{\mu\nu} &= \frac{3q^2 P_1^{\mu\nu} + q^2 g^{\mu\nu} - q^\mu q^\nu}{[q^2 - (v \cdot q)^2]}, & P_3^{\mu\nu} &= \frac{-i \epsilon^{\mu\nu\alpha\beta} q_\alpha v_\beta}{2[q^2 - (v \cdot q)^2]}, \\
P_4^{\mu\nu} &= \frac{g^{\mu\nu} - v^\mu v^\nu + 3P_1^{\mu\nu}}{[q^2 - (v \cdot q)^2]}, & P_5^{\mu\nu} &= \frac{g^{\mu\nu} + 4P_1^{\mu\nu} - P_2^{\mu\nu} - q^2 P_4^{\mu\nu}}{2v \cdot q}.
\end{aligned} \tag{51}$$

The optical theorem relates  $W_{\mu\nu}^{L(R)}$  to the forward scattering amplitude defined as

$$\begin{aligned}
T_{\mu\nu}^L &= \frac{-i}{2m_B} \int d^4x e^{-iq \cdot x} \langle \bar{B} | T J_\mu^{L\dagger}(x) J_\nu^L(0) | \bar{B} \rangle \\
&= -g_{\mu\nu} T_1^L + v_\mu v_\nu T_2^L + i \epsilon_{\mu\nu\alpha\beta} v^\alpha q^\beta T_3^L + q_\mu q_\nu T_4^L + (v_\mu q_\nu + v_\nu q_\mu) T_5^L,
\end{aligned} \tag{52}$$

with an analogous definition for  $T_{\mu\nu}^R$ , giving

$$W_i^L = -\frac{1}{\pi} \text{Im} T_i^L, \quad W_i^R = -\frac{1}{\pi} \text{Im} T_i^R. \tag{53}$$

Contracting the lepton tensor  $L_{L(R)}^{\mu\nu}$  with  $W_{L(R)}^{\mu\nu}$  and neglecting the mass of the leptons give the differential decay rate

$$\frac{d^3\Gamma}{dq^2 dE_- dE_+} = \Gamma_0 \frac{96}{m_B^5} \left[ q^2 W_1 + (2E_- E_+ - q^2/2) W_2 + q^2 (E_- - E_+) W_3 \right] \theta(4E_- E_+ - q^2), \quad (54)$$

where  $E_{\pm} = v \cdot p_{\pm}$ ,  $W_1 = W_1^L + W_1^R$ ,  $W_2 = W_2^L + W_2^R$ ,  $W_3 = W_3^L - W_3^R$  and the normalization factor is

$$\Gamma_0 = \frac{G_F^2 m_B^5}{192\pi^3} \frac{\alpha^2}{16\pi^2} |V_{tb} V_{ts}^*|^2. \quad (55)$$

The  $W_i$  are functions of  $q^2$  and  $v \cdot q = v \cdot (p_+ + p_-)$ . Another quantity of interest is the forward-backward asymmetry in the variable

$$\cos \theta = \frac{v \cdot p_- - v \cdot p_+}{\sqrt{(v \cdot q)^2 - q^2}}, \quad (56)$$

where  $\theta$  is the angle between the  $B$  and  $\ell^+$  in the CM frame of the  $\ell^+ \ell^-$  pair:

$$\frac{d^2 A_{\text{FB}}}{dv \cdot q dq^2} \equiv \int_{-1}^1 d(\cos \theta) \frac{\text{sign}(\cos \theta)}{\Gamma_0} \frac{d^3\Gamma}{dv \cdot q dq^2 d\cos \theta} = \frac{48 q^2}{m_B^5} [(v \cdot q)^2 - q^2] W_3. \quad (57)$$

In terms of the dimensionless variables

$$x_H = \frac{2E_{\ell^-}}{m_B}, \quad \bar{y}_H = \frac{\bar{n} \cdot p_X}{m_B}, \quad u_H = \frac{n \cdot p_X}{m_B}, \quad (58)$$

the triply differential decay rate is

$$\begin{aligned} \frac{1}{\Gamma_0} \frac{d^3\Gamma}{dx_H d\bar{y}_H du_H} &= 24m_B (\bar{y}_H - u_H) \left\{ (1 - u_H)(1 - \bar{y}_H) W_1 + \frac{1}{2} (1 - x_H - u_H)(x_H + \bar{y}_H - 1) W_2 \right. \\ &\quad \left. + \frac{m_B}{2} (1 - u_H)(1 - \bar{y}_H)(2x_H + u_H + \bar{y}_H - 2) W_3 \right\}, \end{aligned} \quad (59)$$

where  $W_i = W_i(u_H, \bar{y}_H)$ . For a strict SCET expansion we want  $n \cdot p_X \ll \bar{n} \cdot p_X$  i.e.  $u_H \ll \bar{y}_H$ . However, it is useful to keep the full dependence on the phase-space prefactors rather than expanding them, because it is then simpler to make contact with the total rate in the local OPE, as emphasized recently in Refs. [53, 54], and so we keep these factors here. We shall also keep the formally subleading kinematic prefactors in our hard functions rather than expanding them as we did in Ref. [37]. Other variables of interest include the dilepton and hadronic invariant masses,

$$y_H = \frac{q^2}{m_B^2}, \quad s_H = \frac{m_X^2}{m_B^2}, \quad (60)$$

where

$$s_H = u_H \bar{y}_H, \quad y_H = (1 - u_H)(1 - \bar{y}_H), \quad (61)$$

so that  $[\bar{y}_H \geq u_H]$

$$\{\bar{y}_H, u_H\} = \frac{1}{2} \left[ 1 - y_H + s_H \pm \sqrt{(1 - y_H + s_H)^2 - 4s_H} \right]. \quad (62)$$

A few interesting doubly differential spectra are

$$\begin{aligned} \frac{1}{\Gamma_0} \frac{d^2\Gamma}{d\bar{y}_H du_H} &= 24m_B(\bar{y}_H - u_H)^2 \left\{ (1 - u_H)(1 - \bar{y}_H)W_1 + \frac{1}{12}(\bar{y}_H - u_H)^2 W_2 \right\}, \\ \frac{1}{\Gamma_0} \frac{d^2\Gamma}{dy_H ds_H} &= 2m_B \sqrt{(1 - y_H + s_H)^2 - 4s_H} \left\{ 12y_H W_1 + [(1 - y_H + s_H)^2 - 4s_H] W_2 \right\}, \\ \frac{1}{\Gamma_0} \frac{d^2\Gamma}{dy_H du_H} &= \frac{2m_B}{(1 - u_H)^3} [(1 - u_H)^2 - y_H]^2 \left\{ 12y_H W_1 + \left[ \frac{(1 - u_H)^2 - y_H}{(1 - u_H)} \right]^2 W_2 \right\}, \\ \frac{1}{\Gamma_0} \frac{d^2\Gamma}{ds_H du_H} &= \frac{2m_B(s_H - u_H^2)^2}{u_H^5} \left\{ 12u_H(1 - u_H)(u_H - s_H)W_1 + (s_H - u_H^2)^2 W_2 \right\}. \end{aligned} \quad (63)$$

For doubly differential forward-backward asymmetries we find

$$\begin{aligned} \frac{d^2 A_{\text{FB}}}{d\bar{y}_H du_H} &= 6m_B^2 (\bar{y}_H - u_H)^3 (1 - u_H)(1 - \bar{y}_H) W_3, \\ \frac{d^2 A_{\text{FB}}}{dy_H ds_H} &= 6m_B^2 y_H [(1 - y_H + s_H)^2 - 4s_H] W_3, \\ \frac{d^2 A_{\text{FB}}}{dy_H du_H} &= 6m_B^2 \frac{y_H [(1 - u_H)^2 - y_H]^3}{(1 - u_H)^4} W_3, \\ \frac{d^2 A_{\text{FB}}}{ds_H du_H} &= 6m_B^2 \frac{(s_H - u_H^2)^3 (u_H - s_H)(1 - u_H)}{u_H^5} W_3. \end{aligned} \quad (64)$$

#### D. LO Matrix Elements in SCET

At lowest order in the  $\Lambda/m_b$  expansion, the only time-ordered product consists of two lowest-order currents  $\mathcal{J}_{\ell\ell}^{(0)}$  as shown in Fig. 4. The factorization of hard contributions into the SCET Wilson coefficients and the decoupling of soft and collinear gluons at lowest order are identical to the steps for  $B \rightarrow X_s \gamma$  and  $B \rightarrow X_u \ell \bar{\nu}$ , and directly give the factorization theorem for these time-ordered products [28]. The SCET result agrees with the factorization theorem of Korchemsky and Sterman [30]. However, the structure of  $\alpha_s(\sqrt{m_b \Lambda})$  and  $\alpha_s(m_b)$  corrections differs from the parton-model rate, as mentioned in Refs. [32, 33]. Beyond lowest order in  $\alpha_s(m_b)$  the kinematic dependences also differ, as mentioned in Ref. [37]. For  $B \rightarrow X_u \ell \bar{\nu}$ , the final triply differential rate with perturbative corrections at  $\mathcal{O}(\alpha_s)$  can be found in Refs. [32, 33].

The factorization and use of the optical theorem is carried out at the scale  $\mu = \mu_i$ , and we expand  $W_i = W_i^{(0)} + W_i^{(2)} + \dots$  in powers of  $\lambda = (\Lambda_{\text{QCD}}/m_b)^{1/2}$  (with no linear term). For  $B \rightarrow X_s \ell^+ \ell^-$  we have bilinear hadronic current operators in SCET in Eq. (19) and so, as is the case for  $B \rightarrow X_u \ell \bar{\nu}$ , we find

$$W_i^{(0)} = h_i(p_X^+, p_X^-, \mu_i) \int_0^{p_X^+} dk^+ \mathcal{J}^{(0)}(p^-, k^+, \mu_i) f^{(0)}(k^+ + \bar{\Lambda} - p_X^+, \mu_i). \quad (65)$$

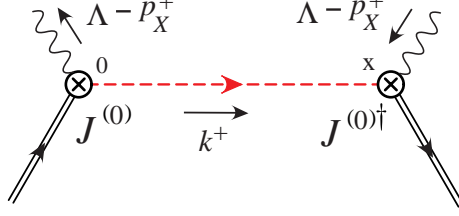


FIG. 4: Time-ordered product for the leading-order factorization theorem.

This result is important, since it states that the same shape function  $f^{(0)}$  appears in  $B \rightarrow X_s \ell^+ \ell^-$  as appears in  $B \rightarrow X_s \gamma$  and  $B \rightarrow X_u \ell \bar{\nu}$ . This formula relies on the power counting  $s \sim y_H \sim \lambda^0$  that we adopted (and would not be true for the counting  $s \sim \lambda^2$  discussed in Appendix B). At tree level the structure of this factorization theorem is illustrated by Fig. 4. The hard coefficients here are

$$\begin{aligned}
h_1(p_X^+, p_X^-, \mu_i) &= \frac{1}{4} \text{Tr} \left[ P_v \bar{\Gamma}_\mu^L \not{n} \Gamma_\nu^L \right] P_1^{\mu\nu} + \frac{1}{4} \text{Tr} \left[ P_v \bar{\Gamma}_\mu^R \not{n} \Gamma_\nu^R \right] P_1^{\mu\nu}, \\
h_2(p_X^+, p_X^-, \mu_i) &= \frac{1}{4} \text{Tr} \left[ P_v \bar{\Gamma}_\mu^L \not{n} \Gamma_\nu^L \right] P_2^{\mu\nu} + \frac{1}{4} \text{Tr} \left[ P_v \bar{\Gamma}_\mu^R \not{n} \Gamma_\nu^R \right] P_2^{\mu\nu}, \\
h_3(p_X^+, p_X^-, \mu_i) &= \frac{1}{4} \text{Tr} \left[ P_v \bar{\Gamma}_\mu^L \not{n} \Gamma_\nu^L \right] P_3^{\mu\nu} - \frac{1}{4} \text{Tr} \left[ P_v \bar{\Gamma}_\mu^R \not{n} \Gamma_\nu^R \right] P_3^{\mu\nu},
\end{aligned} \tag{66}$$

with  $P_v = (1 + \not{n})/2$  and  $\bar{\Gamma} = \gamma^0 \Gamma^\dagger \gamma^0$ . In Eq. (65) we have the same leading-order shape function as in  $B \rightarrow X_s \gamma$  and  $B \rightarrow X_u \ell \bar{\nu}$ , namely

$$\begin{aligned}
f^{(0)}(\ell^+, \mu_i) &= \frac{1}{2} \int \frac{dx^-}{4\pi} e^{-ix^- \ell^+/2} \langle \bar{B}_v | \bar{\mathcal{H}}_v(\tilde{x}) \mathcal{H}_v(0) | \bar{B}_v \rangle \\
&= \frac{1}{2} \langle \bar{B}_v | \bar{h}_v \delta(\ell^+ - in \cdot D) h_v | \bar{B}_v \rangle,
\end{aligned} \tag{67}$$

where  $\tilde{x}^\mu = \bar{n} \cdot x n^\mu / 2$ . This function was first discussed in Ref. [29]. The jet function is defined by  $\mathcal{J}^{(0)}(p^-, k^+) = (-1/\pi) \text{Im} \mathcal{J}_{\omega=p^-}^{(0)}(k^+) \times \theta(p_X^+ - k^+)$ , where

$$i \langle 0 | T [\bar{\chi}_{n,\omega}(0) \frac{\not{n}}{4N_c} \chi_{n,\omega'}(x)] | 0 \rangle = \delta(\omega - \omega') \delta^2(x_\perp) \delta(x^+) \int \frac{dk^+}{2\pi} e^{-ik^+ x^-/2} \mathcal{J}_\omega^{(0)}(k^+), \tag{68}$$

and is known at one-loop order [32, 33], namely

$$\begin{aligned}
\mathcal{J}^{(0)}(p^-, z p_X^+, \mu_i) &= \frac{1}{p_X^+} \left\{ \delta(z) \left[ 1 + \frac{\alpha_s(\mu_i) C_F}{4\pi} \left( 2 \ln^2 \frac{p^- p_X^+}{\mu_i^2} - 3 \ln \frac{p^- p_X^+}{\mu_i^2} + 7 - \pi^2 \right) \right] \right. \\
&\quad \left. + \frac{\alpha_s(\mu_i) C_F}{4\pi} \left[ \left( \frac{4 \ln z}{z} \right)_+ + \left( 4 \ln \frac{p^- p_X^+}{\mu_i^2} - 3 \right) \frac{1}{(z)_+} \right] \theta(z) \right\} \theta(1-z),
\end{aligned} \tag{69}$$

where  $z = k^+ / p_X^+$ . Despite appearances, only the combination  $z p_X^+$  appears in  $\mathcal{J}^{(0)}$  apart from the  $\theta(1-z)$ . This last  $\theta$ -function is induced by the soft function and, when one takes the imaginary part of the full time-ordered product, affects the complex structure. Therefore, we include it in our definition of  $\mathcal{J}^{(0)}(p^-, k^+)$ .

### E. RG Evolution Between $\mu_\Lambda$ and $\mu_i$

The function  $f^{(0)}$  cannot be computed in perturbation theory and must therefore be extracted from data. This same function appears at LO in the  $B \rightarrow X_s \gamma$ ,  $B \rightarrow X_u \ell \bar{\nu}$  and  $B \rightarrow X_s \ell^+ \ell^-$  decay rates. In practice, a model for  $f^{(0)}$  is written down with a few parameters, which are fitted to the data. The support of  $f^{(0)}(\bar{\Lambda} - r^+)$  is  $-\infty$  to  $\bar{\Lambda}$  since  $r^+ \in [0, \infty)$ . It is often convenient to switch variables to  $\hat{f}^{(0)}(r^+) = f^{(0)}(\bar{\Lambda} - r^+)$  which has support from 0 to  $\infty$ , although we shall keep using  $f^{(0)}$  here. A typical three-parameter model is [35, 53]

$$f^{(0)}(\bar{\Lambda} - r^+, \mu_\Lambda) = \hat{f}^{(0)}(r^+, \mu_\Lambda) = \frac{a^b (r^+)^{b-1}}{\Gamma(b) L^b} \exp\left(\frac{-ar^+}{L}\right) \theta(r^+). \quad (70)$$

where  $a, b$  are dimensionless and  $L \sim \Lambda_{\text{QCD}}$ . These parameters can be fitted to the  $B \rightarrow X_s \gamma$  photon spectrum and the function  $f^{(0)}$  can then be used elsewhere. The most natural scale to fix this model is  $\mu = \mu_\Lambda \sim 1 \text{ GeV}$ , at which it contains no large logarithms. The result of evolving the shape function to the intermediate scale is then [33]

$$f^{(0)}(\bar{\Lambda} - r^+, \mu_i) = e^{V_S(\mu_i, \mu_\Lambda)} \frac{1}{\Gamma(\eta)} \int_0^{r^+} dr^{+'} \frac{f^{(0)}(\bar{\Lambda} - r^{+'}, \mu_\Lambda)}{\mu_\Lambda^\eta (r^+ - r^{+'})^{1-\eta}}. \quad (71)$$

(The structure of this result also applies at higher orders in RG-improved perturbation theory [55], and at one-loop a similar structure was considered earlier in Ref. [56].) At NLL order

$$\begin{aligned} V_S(\mu_i, \mu_\Lambda) &= \frac{\Gamma_0^{\text{cusp}}}{2\beta_0^2} \left[ \frac{-4\pi}{\alpha_s(\mu_\Lambda)} (r_2 - 1 - \ln r_2) + \frac{\beta_1}{2\beta_0} \ln^2 r_2 + \left( \frac{\Gamma_1^{\text{cusp}}}{\Gamma_0^{\text{cusp}}} - \frac{\beta_1}{\beta_0} \right) \left( 1 - \frac{1}{r_2} - \ln r_2 \right) \right] \\ &\quad - \frac{\Gamma_0^{\text{cusp}}}{\beta_0} \gamma_E \ln r_2 - \frac{\gamma_0}{\beta_0} \ln r_2, \\ \eta &= \frac{\Gamma_0^{\text{cusp}}}{\beta_0} \ln r_2. \end{aligned} \quad (72)$$

Here,  $r_2 = \alpha_s(\mu_\Lambda)/\alpha_s(\mu_i)$ ,  $\Gamma_0^{\text{cusp}}$  and  $\Gamma_1^{\text{cusp}}$  are the same as in Section II B and  $\gamma_0 = -2C_F$ . For numerical integration this can be rewritten in the form

$$f^{(0)}(\bar{\Lambda} - r^+, \mu_i) = e^{V_S(\mu_i, \mu_\Lambda)} \frac{1}{\Gamma(1 + \eta)} \left( \frac{r^+}{\mu_\Lambda} \right)^\eta \int_0^1 dt f^{(0)}(\bar{\Lambda} - r^+(1 - t^{1/\eta}), \mu_\Lambda). \quad (73)$$

## III. $B \rightarrow X_s \ell^+ \ell^-$ SPECTRA IN THE SHAPE FUNCTION REGION

### A. Triply Differential Spectrum

At lowest order in the power expansion, Eqs. (51) and (65) give the result

$$W_i^{(0)} = h_i(p_X^-, p_X^+, m_b, \mu_i) \int_0^{p_X^+} dk^+ \mathcal{J}^{(0)}(p^-, k^+, \mu_i) f^{(0)}(k^+ + \bar{\Lambda} - p_X^+, \mu_i), \quad (74)$$

where RG evolution from the hard scale to the intermediate scale gives

$$h_i(p_X^-, p_X^+, \mu_i) = U_H(\mu_i, \mu_b) h_i(p_X^-, p_X^+, \mu_b), \quad (75)$$

and the results at  $\mu = \mu_b$  are determined from the traces in Eq. (66):

$$\begin{aligned} h_1(p_X^-, p_X^+, \mu_b) &= \frac{1}{2} \left( |\mathcal{C}_9|^2 + |\mathcal{C}_{10a}|^2 \right) + \frac{2 \operatorname{Re}[\mathcal{C}_7 \mathcal{C}_9^*]}{(1 - \bar{y}_H)} + \frac{2 |\mathcal{C}_7|^2}{(1 - \bar{y}_H)^2}, \\ h_2(p_X^-, p_X^+, \mu_b) &= \frac{2(1 - u_H)}{(\bar{y}_H - u_H)} \left( |\mathcal{C}_9|^2 + |\mathcal{C}_{10a}|^2 + \operatorname{Re}[\mathcal{C}_{10a} \mathcal{C}_{10b}^*] \right) + \frac{|\mathcal{C}_{10b}|^2}{2} - \frac{8 |\mathcal{C}_7|^2}{(1 - \bar{y}_H)(\bar{y}_H - u_H)}, \\ h_3(p_X^-, p_X^+, \mu_b) &= \frac{-4 \operatorname{Re}[\mathcal{C}_{10a} \mathcal{C}_7^*]}{m_B(1 - \bar{y}_H)(\bar{y}_H - u_H)} - \frac{2 \operatorname{Re}[\mathcal{C}_{10a} \mathcal{C}_9^*]}{m_B(\bar{y}_H - u_H)}. \end{aligned} \quad (76)$$

Here  $\mathcal{C}_i = \mathcal{C}_i(p_X^-, p_X^+, \mu_b, \mu_0, m_b)$ , so these hard coefficients also depend on  $m_b$  and have residual  $\mu_0$  scale dependence. Explicit formulae are given in Eq. (33). For convenience we define

$$\begin{aligned} F^{(0)}(p_X^+, p_X^-) &= U_H(\mu_i, \mu_b) \int_0^{p_X^+} dk^+ \mathcal{J}^{(0)}(p^-, k^+, \mu_i) f^{(0)}(k^+ + \bar{\Lambda} - p_X^+, \mu_i) \\ &= p_X^+ U_H(\mu_i, \mu_b) \int_0^1 dz \mathcal{J}^{(0)}(p^-, z p_X^+, \mu_i) f^{(0)}(\bar{\Lambda} - p_X^+(1 - z), \mu_i). \end{aligned} \quad (77)$$

where  $p_X^- = p^- + \bar{\Lambda}$ . In terms of this function,

$$W_i^{(0)} = h_i(p_X^+, p_X^-, \mu_b) F^{(0)}(p_X^+, p_X^-). \quad (78)$$

We find that to NLL

$$\begin{aligned} F^{(0)}(p_X^+, p_X^-) &= U_H(\mu_i, \mu_b) f^{(0)}(\bar{\Lambda} - p_X^+, \mu_i) \\ &+ U_H(\mu_i, \mu_b) \frac{\alpha_s(\mu_i) C_F}{4\pi} \left\{ \left( 2 \ln^2 \frac{p^- p_X^+}{\mu_i^2} - 3 \ln \frac{p^- p_X^+}{\mu_i^2} + 7 - \pi^2 \right) f^{(0)}(\bar{\Lambda} - p_X^+, \mu_i) \right. \\ &\left. + \int_0^1 \frac{dz}{z} \left[ 4 \ln \frac{z p^- p_X^+}{\mu_i^2} - 3 \right] \left[ f^{(0)}(\bar{\Lambda} - p_X^+(1 - z), \mu_i) - f^{(0)}(\bar{\Lambda} - p_X^+, \mu_i) \right] \right\}. \end{aligned} \quad (79)$$

Note that, until we include the  $\alpha_s$  corrections from the jet function,  $F^{(0)}$  is independent of  $p_X^-$ , so that all of this dependence is in the  $h_i(p_X^+, p_X^-, \mu_b)$  functions.

Now, the triply differential decay rate in Eq. (59) becomes

$$\begin{aligned} \frac{1}{\Gamma_0} \frac{d^3 \Gamma}{dx_H d\bar{y}_H du_H} &= 24 m_B (\bar{y}_H - u_H) \left\{ (1 - u_H)(1 - \bar{y}_H) h_1 + \frac{1}{2} (1 - x_H - u_H)(x_H + \bar{y}_H - 1) h_2 \right. \\ &\left. + \frac{m_B}{2} (1 - u_H)(1 - \bar{y}_H)(2x_H + u_H + \bar{y}_H - 2) h_3 \right\} F^{(0)}(m_B u_H, m_B \bar{y}_H), \end{aligned} \quad (80)$$

with  $h_{1,2,3}$  from Eq. (76). As a check on this result, one can make the substitutions

$$\begin{aligned} \mathcal{C}_{9a} = -\mathcal{C}_{10a} &= 1/2, \quad \mathcal{C}_7 = \mathcal{C}_{10b} = 0, \\ \frac{G_F \alpha}{\sqrt{2} \pi} V_{tb} V_{ts}^* &\rightarrow \frac{4 G_F}{\sqrt{2}} V_{ub}, \end{aligned} \quad (81)$$

after which the  $h_1$  and  $h_2$  terms in Eq. (80) agree with terms in the leading-order shape-function spectrum for  $B \rightarrow X_u \ell \bar{\nu}$  [32, 57]. The  $h_3$  term for  $B \rightarrow X_s \ell \ell$  was the difference of products of left- and right-handed currents and so should not agree in this limit.

### B. $d^2\Gamma/dq^2 dm_X^2$ Spectrum with $q^2$ and $m_X$ Cuts

Next we discuss doubly differential rates and forward-backward (F.B.) asymmetries. For  $d^2\Gamma/dq^2 dm_X^2$  the rate is obtained from Eq. (80) by integrating over  $x_H$  and changing variables. In terms of dimensionless variables  $y_H = q^2/m_B^2$  and  $s_H = m_X^2/m_B^2$  we have

$$\begin{aligned} \frac{1}{\Gamma_0} \frac{d^2\Gamma}{dy_H ds_H} &= H^{ys}(y_H, s_H) m_B F^{(0)}\left(m_B u_H(y_H, s_H), m_B \bar{y}_H(y_H, s_H)\right), \\ \frac{1}{\Gamma_0} \frac{d^2 A_{\text{FB}}}{dy_H ds_H} &= K^{ys}(y_H, s_H) m_B F^{(0)}\left(m_B u_H(y_H, s_H), m_B \bar{y}_H(y_H, s_H)\right), \end{aligned} \quad (82)$$

where

$$\begin{aligned} H^{ys}(y_H, s_H) &= 2\sqrt{(1-y_H+s_H)^2-4s_H} \left\{ 12y_H h_1 + [(1-y_H+s_H)^2-4s_H] h_2 \right\}, \\ K^{ys}(y_H, s_H) &= 6y_H [(1-y_H+s_H)^2-4s_H] h_3 \end{aligned} \quad (83)$$

and we need to substitute  $h_{1,2,3}$  from Eq. (76) and  $u_H(y_H, s_H)$  and  $\bar{y}_H(y_H, s_H)$ , as given in Eq. (62). When one takes experimental cuts on  $q^2$  and  $m_X^2$ ,

$$y_H^{\min} < y_H < y_H^{\max}, \quad 0 < s_H < s_H^0, \quad (84)$$

the limits on the doubly differential rate and F.B. asymmetry in Eq. (82) are

$$\begin{aligned} 1) \quad & y_H^{\min} \leq y_H \leq y_H^{\max}, & 0 \leq s_H \leq \min\{s_H^0, (1-\sqrt{y_H})^2\}, \\ 2) \quad & 0 \leq s_H \leq s_H^0, & y_H^{\min} \leq y_H \leq \min\{y_H^{\max}, (1-\sqrt{s_H})^2\}, \end{aligned} \quad (85)$$

depending on the desired order of integration.

### C. $d^2\Gamma/dm_X^2 dp_X^\dagger$ Spectrum with $q^2$ and $m_X$ Cuts

The hadronic invariant-mass spectrum and forward-backward asymmetry can be obtained by integrating the doubly differential spectra

$$\begin{aligned} \frac{1}{\Gamma_0} \frac{d^2\Gamma}{ds_H du_H} &= H^s(s_H, u_H) m_B F^{(0)}\left(m_B u_H, m_B \frac{s_H}{u_H}\right), \\ \frac{1}{\Gamma_0} \frac{d^2 A_{\text{FB}}}{ds_H du_H} &= K^s(s_H, u_H) m_B F^{(0)}\left(m_B u_H, m_B \frac{s_H}{u_H}\right) \end{aligned} \quad (86)$$

over  $u_H$ . Here

$$\begin{aligned}
H^s(s_H, u_H) &= \frac{4(s_H - u_H^2)^2}{(u_H - s_H)u_H^4} \left\{ (1 - u_H)(u_H - s_H)(3u_H - 2s_H - u_H^2)(|\mathcal{C}_9|^2 + |\mathcal{C}_{10a}|^2) \right. \\
&\quad + 4u_H(3u_H - s_H - 2u_H^2)|\mathcal{C}_7|^2 + 12u_H(1 - u_H)(u_H - s_H)\text{Re}[\mathcal{C}_7\mathcal{C}_9^*] \\
&\quad + (1 - u_H)(u_H - s_H)(s_H - u_H^2)\text{Re}[\mathcal{C}_{10a}\mathcal{C}_{10b}^*] + \frac{(u_H - s_H)(s_H - u_H^2)^2}{4u_H} |\mathcal{C}_{10b}|^2 \left. \right\}, \\
K^s(s_H, u_H) &= \frac{-12(s_H - u_H^2)^2(u_H - s_H)(1 - u_H)}{u_H^4} \left\{ \text{Re}[\mathcal{C}_9\mathcal{C}_{10a}^*] + \frac{2u_H}{u_H - s_H} \text{Re}[\mathcal{C}_7\mathcal{C}_{10a}^*] \right\},
\end{aligned} \tag{87}$$

and the limits with  $q^2$  and  $m_X$  cuts are

$$\begin{aligned}
0 \leq s_H \leq s_H^0, \quad \max\{s_H, u_1(s_H)\} \leq u_H \leq \min\{\sqrt{s_H}, u_2(s_H)\}, \\
u_1(s_H) &= \frac{1 + s_H - y_H^{\min} - \sqrt{(1 + s_H - y_H^{\min})^2 - 4s_H}}{2}, \\
u_2(s_H) &= \frac{1 + s_H - y_H^{\max} - \sqrt{(1 + s_H - y_H^{\max})^2 - 4s_H}}{2}.
\end{aligned} \tag{88}$$

#### D. $d^2\Gamma/dq^2 dp_X^+$ Spectrum with $q^2$ and $m_X$ Cuts

From Eqs. (63) and the above results, we can obtain the dilepton invariant-mass spectrum and forward-backward asymmetry, for example by integrating the doubly differential spectra

$$\begin{aligned}
\frac{1}{\Gamma_0} \frac{d^2\Gamma}{dy_H du_H} &= H^y(y_H, u_H) m_B F^{(0)}\left(m_B u_H, m_B \frac{1 - y_H - u_H}{1 - u_H}\right), \\
\frac{1}{\Gamma_0} \frac{d^2 A_{\text{FB}}}{dy_H du_H} &= K^y(y_H, u_H) m_B F^{(0)}\left(m_B u_H, m_B \frac{1 - y_H - u_H}{1 - u_H}\right)
\end{aligned} \tag{89}$$

over  $u_H$ . Here

$$\begin{aligned}
H^y(y_H, u_H) &= \frac{4[(1 - u_H)^2 - y_H]^2}{y_H(1 - u_H)^3} \left\{ y_H[(1 - u_H)^2 + 2y_H] (|\mathcal{C}_9|^2 + |\mathcal{C}_{10a}|^2) \right. \\
&\quad + [8(1 - u_H)^2 + 4y_H] |\mathcal{C}_7|^2 + 12y_H(1 - u_H)\text{Re}[\mathcal{C}_7\mathcal{C}_9^*] \\
&\quad + y_H[(1 - u_H)^2 - y_H] \text{Re}[\mathcal{C}_{10a}\mathcal{C}_{10b}^*] + \frac{y_H[(1 - u_H)^2 - y_H]^2}{4(1 - u_H)^2} |\mathcal{C}_{10b}|^2 \left. \right\}, \\
K^y(y_H, u_H) &= \frac{-12y_H [(1 - u_H)^2 - y_H]^2}{(1 - u_H)^3} \left\{ \text{Re}[\mathcal{C}_9\mathcal{C}_{10a}^*] + \frac{2(1 - u_H)}{y_H} \text{Re}[\mathcal{C}_7\mathcal{C}_{10a}^*] \right\},
\end{aligned} \tag{90}$$

and the limits of integration with cuts are

$$y_H^{\min} < y_H < y_H^{\max}, \quad 0 \leq u_H \leq \min\left\{1 - \sqrt{y_H}, \frac{1 + s_H^0 - y_H - \sqrt{(1 + s_H^0 - y_H)^2 - 4s_H^0}}{2}\right\}. \tag{91}$$

The opposite order of integration is also useful:

$$0 \leq u_H \leq 1, \quad y_1(u_H) < y_H < y_2(u_H),$$

$$y_1(u_H) = \max \left\{ y_H^{\min}, \frac{(1-u_H)(u_H-s_H^0)}{u_H} \right\}, \quad y_2(u_H) = \min \left\{ y_H^{\max}, (1-u_H)^2 \right\}. \quad (92)$$

The doubly differential rate can also be expressed in terms of the coefficients  $C_9^{\text{mix}}$ ,  $C_7^{\text{mix}}$ , and  $C_{10}$ . This is one step closer to the short-distance coefficients  $C_9$ ,  $C_7$ , and  $C_{10}$  of  $H_W$ , which we wish to measure in order to test the Standard Model predictions for the corresponding FCNC interactions. Substituting Eq. (33) into Eq. (90) gives

$$H^y(y_H, u_H) = \frac{4[(1-u_H)^2 - y_H]^2}{(1-u_H)^3} \left\{ |C_7^{\text{mix}}(s, \mu_0)|^2 \left[ 4\Omega_C^2(s, \mu_b) + \frac{8(1-u_H)^2}{y_H} \Omega_D^2(s, \mu_b) \right] \right.$$

$$+ [ |C_9^{\text{mix}}(s, \mu_0)|^2 + C_{10}^2 ] \left[ 2y_H \Omega_A^2(s, \mu_b) + (1-u_H)^2 \Omega_B^2(y_H, u_H, s, \mu_b) \right]$$

$$\left. + \text{Re} [ C_7^{\text{mix}}(s, \mu_0) C_9^{\text{mix}}(s, \mu_0)^* ] \left[ 12(1-u_H) \Omega_E(s, \mu_b) \right] \right\}$$

$$K^y(y_H, u_H) = \frac{-12y_H [(1-u_H)^2 - y_H]^2}{(1-u_H)^3} \left\{ \text{Re} [ C_9^{\text{mix}}(s, \mu_0) C_{10}^* ] \Omega_A^2(s, \mu_b) \right.$$

$$\left. + \frac{2(1-u_H)}{y_H} \text{Re} [ C_7^{\text{mix}}(s, \mu_0) C_{10}^* ] \Omega_A(s, \mu_b) \Omega_D(s, \mu_b) \right\}, \quad (93)$$

where  $s = q^2/m_b^2$  and

$$\Omega_A = 1 + \frac{\alpha_s(\mu_b)}{\pi} \omega_a^V(s, \mu_b), \quad (94)$$

$$\Omega_B = 1 + \frac{\alpha_s(\mu_b)}{\pi} \left[ \omega_a^V(s, \mu_b) + \omega_c^V(s, \mu_b) + \frac{(1-u_H)^2 - y_H}{2(1-u_H)^2} \omega_b^V(s, \mu_b) \right],$$

$$\Omega_C = 1 + \frac{\alpha_s(\mu_b)}{\pi} \left[ \omega_a^T(s, \mu_b) - \omega_b^T(s, \mu_b) - \omega_d^T(s, \mu_b) \right],$$

$$\Omega_D = 1 + \frac{\alpha_s(\mu_b)}{\pi} \left[ \omega_a^T(s, \mu_b) - \omega_c^T(s, \mu_b) - \frac{(1-u_H)^2 + y_H}{2(1-u_H)^2} \omega_b^T(s, \mu_b) \right],$$

$$\Omega_E = (2\Omega_A \Omega_D + \Omega_B \Omega_C) / 3. \quad (95)$$

This is the form that turned out to be the most useful for the analysis in Ref. [44].

## E. Numerical Analysis of Wilson Coefficients

As shown in Fig. 1, for the small- $q^2$  window ( $q^2 < 6 \text{ GeV}^2$ ) we have  $p_X^+ \ll p_X^-$ . Generically, the hard contributions in  $C_9$ ,  $C_7$ , and  $C_{10a,10b}$  from our split-matching procedure depend on the variable  $q^2$ . In Fig. 5 we plot the  $q^2$  dependence of the real part of the coefficients and see that there is in fact very little numerical change over the low- $q^2$  window. Here  $\text{Re}[C_9^{\text{local}}]$  varies by  $\pm 1.5\%$ ,  $\text{Re}[C_9^{\text{mix}}]$  by  $\pm 1\%$ , and the real parts of  $\{C_9, C_7, C_{10a}, C_{10b}\}$  by  $\{\pm 1\%, \pm 5\%, \pm 2\%, \pm 3\%\}$ . The imaginary parts are either very small or also change by only a few percent over the low- $q^2$  window. The analytic formulae for the  $q^2$  dependence mean

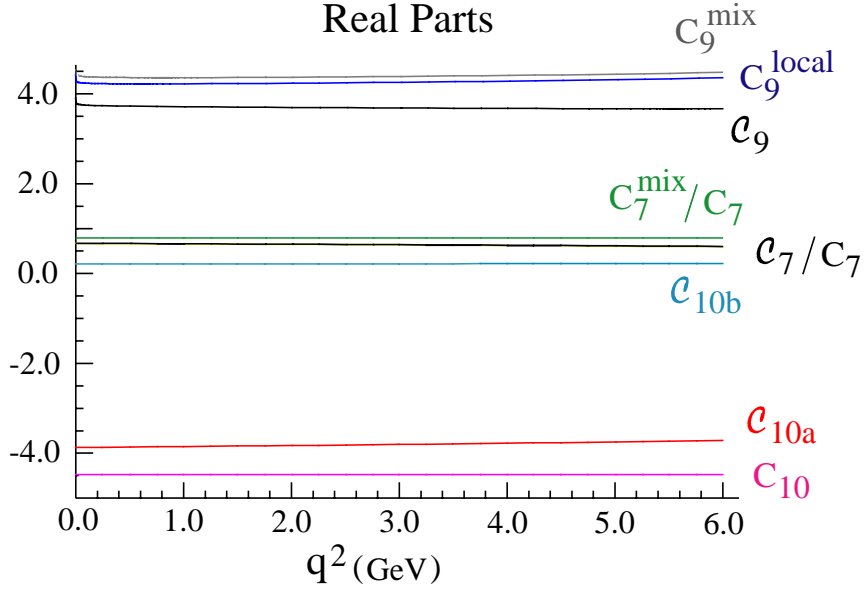


FIG. 5: Comparison of the real part of Wilson coefficients at  $\mu_0 = \mu_b = 4.8 \text{ GeV}$  with  $m_c/m_b = 0.292$ ,  $\overline{m}_b(\mu_0) = 4.17 \text{ GeV}$ , and  $m_b = 4.8 \text{ GeV}$ . For  $C_9$ ,  $C_7$ , and  $C_{10b}$  we take  $p_X^+ = 0$ .

that there is no problem keeping the exact dependence, but this does make it necessary to perform integrals over regions in  $q^2$  numerically. A reasonable first approximation can actually be obtained by fixing a constant  $q^2$  in the hard coefficients, while keeping the full  $q^2$  dependence elsewhere.

Since the coefficients change very little with  $q^2$  we continue our numerical analysis by fixing  $q^2 = 3 \text{ GeV}^2$ . If we then take  $\mu_0 = \mu_b = m_b = 4.8 \text{ GeV}$ ,  $\overline{m}_b(\mu_0) = 4.17 \text{ GeV}$ ,  $m_c/m_b = 0.292$  and  $p_X^+ = 0$  we find that Eq. (33) gives

$$\begin{aligned}
 C_9 &= 0.826 C_9^{\text{mix}} + 0.097 C_7^{\text{mix}} = 3.448 \frac{C_9^{\text{mix}}}{C_9^{\text{NDR}}} - 0.030 \frac{C_7^{\text{mix}}}{C_7^{\text{NDR}}}, \\
 C_7 &= 0.823 C_7^{\text{mix}} + 0.001 C_9^{\text{mix}} = -0.239 \frac{C_7^{\text{mix}}}{C_7^{\text{NDR}}} + 0.005 \frac{C_9^{\text{mix}}}{C_9^{\text{NDR}}}.
 \end{aligned} \tag{96}$$

These numbers indicate that, despite the entanglement of  $C_{7,9}^{\text{mix}}$  in  $C_{7,9}$  due to  $\alpha_s(m_b)$  corrections, numerically  $C_9$  is dominated by  $C_9$  and  $C_7$  is dominated by  $C_7$  in the Standard Model.

For the coefficients at  $q^2 = 3.0 \text{ GeV}^2$ , with the other parameters as above, we have

$$\begin{aligned}
 C_9^{\text{mix}} &= 4.487 + 0.046i, & C_7^{\text{mix}} &= -0.248, \\
 C_9(u_H = 0) &= 3.683 + 0.038i, & C_7(u_H = 0) &= -0.198 + 6 \times 10^{-5}i, \\
 C_9(u_H = 0.2) &= 3.663 + 0.038i, & C_7(u_H = 0.2) &= -0.193 + 10^{-4}i, \\
 C_{10a} &= -3.809, & C_{10b}(u_H = 0) &= 0.214, \\
 & & C_{10b}(u_H = 0.2) &= 0.237.
 \end{aligned} \tag{97}$$

The relevant range of  $p_X^+$  in Fig. 1 gives  $0 \leq u_H \leq 0.2$ . From the above numbers it is easy to see that the  $u_H$  dependence of  $C_9$ ,  $C_7$ , and  $C_{10b}$  is very mild over the range of interest. The perturbative  $\alpha_s$  corrections due to  $\omega_i^{V,T}$  reduce both  $C_9$  and  $C_7$  by 17% relative to  $C_9^{\text{mix}}$

and  $C_7^{\text{mix}}$  respectively, and  $C_{10a}$  by 15%. This can be seen both in Fig. 5 and in Eq. (97), when one notes that  $C_{10} = -4.480$ . Comparing with coefficients in the local OPE, we note that the  $\omega_{\text{semi}}^{\text{OPE}}$  factor, which accounts for the difference between  $C_9^{\text{local}}$  and  $C_9^{\text{mix}}$ , is significantly smaller than the combination of  $\alpha_s$  corrections in the  $\omega_i^V$  terms that shifts  $C_9$  from its lowest-order value.

In quoting the above numbers, we have not varied the scales  $\mu_0$  and  $\mu_b$ . The main point was to compare the size of the hard corrections in the shape function and local OPE regions, and to see how much deviation from  $C_{7,9}^{\text{mix}}$  they cause. The dependence on  $\mu_0$  for the  $C_i$  is similar to that in the local OPE analysis at NLL [9, 10] and will be reduced by a similar amount when the full NNLL expressions are included in  $C_{7,9}^{\text{mix}}$ . The  $\mu_b$  dependence of the  $C_i$  is fairly strong because of the appearance of double logarithms, but it is canceled by the  $\mu_b$  dependence in the function  $F^{(0)}$ , which contains the NLL jet and shape functions.

#### IV. CONCLUSION

In this paper we have performed a model-independent analysis of  $B \rightarrow X_s \ell^+ \ell^-$  decays with cuts giving the small- $q^2$  window and an  $m_X$  cut to remove  $b \rightarrow c$  backgrounds. These cuts put us in the shape function region. We analyzed the rate for the formal counting with  $q^2 \sim \lambda^0$  and  $m_X^2 \sim \lambda^2$  and showed that the same universal shape function as in  $B \rightarrow X_u \ell \bar{\nu}$  and  $B \rightarrow X_s \gamma$  is the only non-perturbative input needed for these decays. We also developed a new effective-theory technique of split matching. Split matching between two effective theories is done not at a single scale  $\mu$ , but rather at two nearby scales. For  $B \rightarrow X_s \ell^+ \ell^-$  this allowed us to decouple the perturbation-theory analysis above and below  $m_b$ , which simplifies the organization of the  $\alpha_s$  contributions.

In Section III we presented the leading power triply differential spectrum and doubly differential forward-backward asymmetry with renormalization-group evolution and matching to  $\mathcal{O}(\alpha_s)$ . Above the scale  $m_b$ , we restricted our analysis to include the standard NLL terms from the local OPE, but illustrated how terms from NNLL can be incorporated. Below  $m_b$  we considered running to NLL and matching at one-loop (NNLL evolution will be straightforward to incorporate if desired). We then computed several phenomenologically relevant doubly differential spectra with phase-space cuts on  $q^2$  and  $m_X$  (from which the singly differential spectra can be obtained by numerical integration). In section III E we discussed the numerical size of our perturbative hard coefficients and compared them to the local OPE results.

Our results for the doubly differential rate in Eqs. (89,90) together with  $F^{(0)}$  from Eq. (79) determine the shape function dependent rate for  $B \rightarrow X_s \ell^+ \ell^-$ . Using as input a result for the non-perturbative shape function  $f^{(0)}$  from a fit to the  $B \rightarrow X_s \gamma$  spectrum or from  $B \rightarrow X_u \ell \bar{\nu}$  gives a model-independent result for  $B \rightarrow X_s \ell^+ \ell^-$  with phase space cuts. A full investigation of the  $m_X$ -cut dependence and phenomenology is carried out in a companion publication [44]. An intriguing universality of the cut dependence is found, which makes the experimental extraction of short-distance Wilson coefficients in the presence of cuts much simpler. An extension of the analysis of this paper to include subleading shape-function effects will be presented in the near future [58].

## Acknowledgments

We thank Z. Ligeti and F. Tackmann for helpful discussions and for collaboration on a related analysis of  $B \rightarrow X_s \ell \ell$ , and D. Pirjol for comments on the manuscript. This work was supported in part by the U.S. Department of Energy (DOE) under the cooperative research agreement DF-FC02-94ER40818 and by the Office of Nuclear Science. I.S. was also supported in part by the DOE Outstanding Junior Investigator program and the Sloan foundation.

## APPENDIX A: WILSON COEFFICIENTS

The coefficients and functions that appear in Eq. (6) are defined as follows [9].

$$\begin{aligned}
C_7(M_W) &= -\frac{1}{2}A(m_t^2/M_W^2), \\
C_8(M_W) &= -\frac{1}{2}F(m_t^2/M_W^2), \\
Y(x) &= C(x) - B(x), \\
Z(x) &= C(x) + \frac{1}{4}D(x), \\
A(x) &= \frac{x(8x^2 + 5x - 7)}{12(x-1)^3} + \frac{x^2(2-3x)}{2(x-1)^4} \ln x, \\
B(x) &= \frac{x}{4(1-x)} + \frac{x}{4(x-1)^2} \ln x, \\
C(x) &= \frac{x(x-6)}{8(x-1)} + \frac{x(3x+2)}{8(x-1)^2} \ln x, \\
D(x) &= \frac{-19x^3 + 25x^2}{36(x-1)^3} + \frac{x^2(5x^2 - 2x - 6)}{18(x-1)^4} \ln x - \frac{4}{9} \ln x, \\
E(x) &= \frac{x(18 - 11x - x^2)}{12(1-x)^3} + \frac{x^2(15 - 16x + 4x^2)}{6(1-x)^4} \ln x - \frac{2}{3} \ln x, \\
F(x) &= \frac{x(x^2 - 5x - 2)}{4(x-1)^3} + \frac{3x^2}{2(x-1)^4} \ln x,
\end{aligned}$$

and

$$\begin{aligned}
t_i &= (2.2996, -1.0880, -\frac{3}{7}, -\frac{1}{14}, -0.6494, -0.0380, -0.0186, -0.0057), \\
a_i &= (\frac{14}{23}, \frac{16}{23}, \frac{6}{23}, -\frac{12}{23}, 0.4086, -0.4230, -0.8994, 0.1456), \\
p_i &= (0, 0, -\frac{80}{203}, \frac{8}{33}, 0.0433, 0.1384, 0.1648, -0.0073), \\
\rho_i^{NDR} &= (0, 0, 0.8966, -0.1960, -0.2011, 0.1328, -0.0292, -0.1858), \\
s_i &= (0, 0, -0.2009, -0.3579, 0.0490, -0.3616, -0.3554, 0.0072), \\
q_i &= (0, 0, 0, 0, 0.0318, 0.0918, -0.2700, 0.0059).
\end{aligned}$$

## APPENDIX B: THE CASE OF COLLINEAR $q^2$

In the body of the paper we used  $q^2 \sim \lambda^0$ . We were free to choose this counting since the power counting for the leptonic variable  $q^2$  does not affect the counting for  $p_X^\pm$  in the

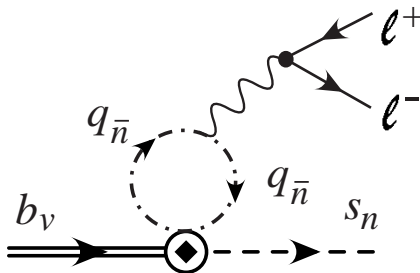


FIG. 6: Additional graphs in SCET for the matching computation for the case where  $q^2 \sim \lambda^2$ .

shape function region. (The only restriction was not to have  $q^2$  too close to  $m_b^2$ .) However, we are free to consider other choices. In this appendix we consider how our analysis will change if we instead take  $q^2 \sim \lambda^2$ . With this scaling, new physical degrees of freedom are needed at leading order in SCET, making the analysis more complicated. In particular we must consider graphs with quark fields that are collinear to the collinear photon (or dilepton pair), since with this power counting we have  $(q^0)^2 \gg q^2$ .

An example of a new *nonzero* graph is the one generated by four-quark operators within SCET, as shown in Fig. 6, which involve these additional degrees of freedom. In this graph we have a light-quark loop of collinear- $\bar{n}$  fields that are collinear to the virtual photon. The presence of this type of diagram changes the hard matching at  $\mu_b = m_b$ . It also means that we have a more complicated pattern of operator mixing within SCET, since divergences in the displayed diagram will cause an evolution for  $C_9$ , etc. Therefore, the running below  $m_b$  will no longer be universal. In the presence of these diagrams the jet function will also no longer be given by a single bilinear operator, since it will also involve some contributions with a factorized matrix element of  $\bar{n}$ -fields, which are also integrated out at  $p^2 \sim m_b \Lambda_{\text{QCD}}$ . Finally, the appearance of these additional degrees of freedom might also affect the number of non-perturbative shape functions that appear in the factorization theorem. It would be interesting to carry out a detailed analysis of this  $q^2 \sim \lambda^2$  case in the future.

In  $B \rightarrow X_s \gamma$  at lowest order, the analog of the graph in Fig. 6 vanishes at one-loop order, and this argument can be extended to include higher orders in  $\alpha_s$  [43]. This relies on the fact that here  $q^2 = 0$  and does not generate a scale. We find that the same reasoning does not apply for  $B \rightarrow X_s \ell \ell$  for parametrically small but finite  $q^2$ .

Finally, we comment on the possibility of penguin charm-loop effects. In our analysis we integrated out the charm loops at the same time as the bottom loops. This is reasonable when treating  $q^2 \sim \lambda^0$ . One could also consider the case  $m_c^2 \sim m_b \Lambda$ , which is also reasonable numerically. This type of power counting was considered for the simpler case of  $B \rightarrow X_c \ell \bar{\nu}$  decays with energetic  $X_c$  in Ref. [59] and it would be interesting to extend this to  $B \rightarrow X_s \ell \ell$ . We remark that the problematic region for  $B \rightarrow \pi \pi$  factorization theorems [60, 61, 62, 63], which is near the charm threshold,  $q^2 \sim 4m_c^2$ , is not relevant for our analysis. The experimental cuts on  $q^2$  explicitly remove the known large contributions from this region.

- 
- [1] CLEO Collaboration, M. S. Alam *et al.*, Phys. Rev.Lett. **74**, 2885 (1995).
  - [2] ALEPH Collaboration, R. Barate *et al.*, Phys. Lett. **B429**, 169 (1998).
  - [3] Belle Collaboration, K. Abe *et al.*, Phys. Lett. **B511**, 151 (2001) [arXiv:hep-ex/0103042].

- [4] CLEO Collaboration, S. Chen *et al.*, Phys. Rev. Lett. **87**, 251807 (2001) [arXiv:hep-ex/0108032].
- [5] BABAR Collaboration, B. Aubert *et al.* [arXiv:hep-ex/0207074].
- [6] Belle Collaboration, J. Kaneko *et al.*, Phys. Rev. Lett. **90**, 021801 (2003) [arXiv:hep-ex/0208029].
- [7] BABAR Collaboration, B. Aubert *et al.*, arXiv:hep-ex/0308016; BABAR Collaboration, B. Aubert *et al.*, Phys. Rev. Lett. **93**, 081802 (2004) [arXiv:hep-ex/0404006].
- [8] B. Grinstein, M. Savage and M. B. Wise, Nucl. Phys. **B319**, 271 (1989).
- [9] A. J. Buras and M. Münz, Phys. Rev. **D52**, 186 (1995), [arXiv:hep-ph/9501281].
- [10] M. Misiak, Nucl. Phys. **B393**, 23 (1993); **B439**, 461(E) (1995).
- [11] C. Bobeth, M. Misiak and J. Urban, Nucl. Phys. **B574**, 291 (2000) [arXiv:hep-ph/9910220]; K. G. Chetyrkin, M. Misiak and M. Munz, Phys. Lett. B **400**, 206 (1997) [Erratum-ibid. B **425**, 414 (1998)] [arXiv:hep-ph/9612313].
- [12] H. H. Asatryan, H. M. Asatrian, C. Greub and M. Walker, Phys. Rev **D65**, 074004 (2002), [arXiv:hep-ph/0109140]; H. M. Asatrian, H. H. Asatryan, A. Hovhannisyan and V. Poghosyan, Mod. Phys. Lett. A **19**, 603 (2004) [arXiv:hep-ph/0311187].
- [13] A. Ghinculov, T. Hurth, G. Isidori and Y.-P. Yao, Nucl. Phys. **B648**, 254 (2003) [arXiv:hep-ph/0208088]; H. M. Asatrian, K. Bieri, C. Greub and A. Hovhannisyan, Phys. Rev. **D66**, 094013 (2002) [arXiv:hep-ph/0209006].
- [14] C. Bobeth, P. Gambino, M. Gorbahn and U. Haisch, JHEP **0404**, 071 (2004) [arXiv:hep-ph/0312090].
- [15] A. Ghinculov, T. Hurth, G. Isidori and Y.-P. Yao, Nucl. Phys. **B685**, 351 (2004) [arXiv:hep-ph/0312128]; A. Ghinculov, T. Hurth, G. Isidori and Y.-P. Yao, Nucl. Phys. Proc. Suppl. **116**, 284 (2003) [arXiv:hep-ph/0211197].
- [16] M. A. Shifman and M. B. Voloshin, Sov. J. Nucl. Phys. **41**, 120 (1985); J. Chay, H. Georgi and B. Grinstein, Phys. Lett. B **247**, 399 (1990); I. I. Y. Bigi, N. G. Uraltsev and A. I. Vainshtein, Phys. Lett. B **293**, 430 (1992) [Erratum-ibid. B **297**, 477 (1993)]; A. V. Manohar and M. B. Wise, Phys. Rev. D **49**, 1310 (1994).
- [17] A. V. Manohar and M. B. Wise, Cambridge Monogr. Part. Phys. Nucl. Phys. Cosmol. **10**, 1 (2000).
- [18] A. F. Falk, M. E. Luke and M. J. Savage, Phys. Rev. **D49**, 3367 (1994) [arXiv:hep-ph/9308288].
- [19] A. Ali, G. Hiller, L. T. Handoko and T. Morozumi, Phys. Rev. **D55**, 4105 (1997) [arXiv:hep-ph/9609449].
- [20] C. W. Bauer and C. N. Burrell, Phys. Rev. **D62**, 114028 (2000) [arXiv:hep-ph/9911404]; Phys. Lett. **B469**, 248 (1999) [arXiv:hep-ph/9907517].
- [21] F. Krüger and L. M. Sehgal, Phys. Lett. **B380**, 199 (1996) [arXiv:hep-ph/9603237].
- [22] J. W. Chen, G. Rupak and M. J. Savage, Phys. Lett. B **410**, 285 (1997) [arXiv:hep-ph/9705219]; G. Buchalla, G. Isidori and S.-J. Rey, Nucl. Phys. **B511**, 594 (1998) [arXiv:hep-ph/9705253].
- [23] B. Aubert *et al.* [BABAR Collaboration], Phys. Rev. Lett. **93**, 081802 (2004) [arXiv:hep-ex/0404006]. M. Iwasaki [Belle Collaboration], arXiv:hep-ex/0503044. B. Aubert *et al.* [BABAR Collaboration], arXiv:hep-ex/0308016. J. Kaneko *et al.* [Belle Collaboration], Phys. Rev. Lett. **90**, 021801 (2003) [arXiv:hep-ex/0208029].
- [24] A. Ali and G. Hiller, Phys. Rev. **D58**, 074001 (1998) [arXiv:hep-ph/9803428]; Phys. Rev. D **60**, 034017 (1999) [arXiv:hep-ph/9807418].

- [25] C. W. Bauer, S. Fleming and M. E. Luke, Phys. Rev. **D63**, 014006 (2001) [arXiv:hep-ph/0005275].
- [26] C. W. Bauer, S. Fleming, D. Pirjol and I. W. Stewart, Phys. Rev. **D63**, 114020 (2001) [arXiv:hep-ph/0011336].
- [27] C. W. Bauer and I. W. Stewart, Phys. Lett. B **516**, 134 (2001) [arXiv:hep-ph/0107001].
- [28] C. W. Bauer, D. Pirjol and I. W. Stewart, Phys. Rev. **D65**, 054022 (2002) [arXiv:hep-ph/0109045].
- [29] M. Neubert, Phys. Rev. D **49** (1994) 3392 [hep-ph/9311325]; *ibid.* 4623 [hep-ph/9312311]; I. I. Y. Bigi *et al.*, Int. J. Mod. Phys. A **9** (1994) 2467 [hep-ph/9312359].
- [30] G. P. Korchemsky and G. Sterman, Phys. Lett. **B340**, 96 (1994) [arXiv:hep-ph/9407344].
- [31] T. Mannel and S. Recksiegel, Phys. Rev. D **63**, 094011 (2001) [arXiv:hep-ph/0009268].
- [32] C. W. Bauer and A. V. Manohar, Phys. Rev. **D70**, 034024 (2004) [arXiv:hep-ph/0312109].
- [33] S. W. Bosch, B. O. Lange, M. Neubert and G. Paz, Nucl. Phys. **B699**, 335 (2004) [arXiv:hep-ph/0402094].
- [34] C. W. Bauer, M. E. Luke and T. Mannel, Phys. Rev. **D68**, 094001 (2003) [arXiv:hep-ph/0102089].
- [35] A. K. Leibovich, Z. Ligeti and M. B. Wise, Phys. Lett. B **539**, 242 (2002) [arXiv:hep-ph/0205148].
- [36] C. W. Bauer, M. E. Luke and T. Mannel, Phys. Lett. **B543**, 261 (2002) [arXiv:hep-ph/0205150].
- [37] K. S. M. Lee and I. W. Stewart, Nucl. Phys. **B721**, 325 (2005) [arXiv:hep-ph/0409045].
- [38] S. W. Bosch, M. Neubert and G. Paz, JHEP **0411**, 073 (2004) [arXiv:hep-ph/0409115].
- [39] M. Beneke, F. Campanario, T. Mannel and B. D. Pecjak, JHEP **0506**, 071 (2005) [arXiv:hep-ph/0411395].
- [40] B. O. Lange, arXiv:hep-ph/0511098.
- [41] A. K. Leibovich and I. Z. Rothstein, Phys. Rev. D **61**, 074006 (2000) [arXiv:hep-ph/9907391].
- [42] A. K. Leibovich, I. Low and I. Z. Rothstein, Phys. Rev. D **62**, 014010 (2000) [arXiv:hep-ph/0001028].
- [43] M. Neubert, Eur. Phys. J. C **40**, 165 (2005) [arXiv:hep-ph/0408179].
- [44] K. S. M. Lee, Z. Ligeti, I. W. Stewart, F. J. Tackmann, arXiv:hep-ph/0512191.
- [45] A. K. Leibovich, I. Low and I. Z. Rothstein, Phys. Rev. D **62**, 014010 (2000) [arXiv:hep-ph/0001028]; Phys. Rev. D **61**, 053006 (2000) [arXiv:hep-ph/9909404]; A. K. Leibovich and I. Z. Rothstein, Phys. Rev. D **61**, 074006 (2000) [arXiv:hep-ph/9907391].
- [46] J. Chay, C. Kim and A. K. Leibovich, Phys. Rev. D **72**, 014010 (2005) [arXiv:hep-ph/0505030].
- [47] B. Grinstein and D. Pirjol, arXiv:hep-ph/0505155.
- [48] C. Greub, T. Hurth and D. Wyler, Phys. Rev. D **54**, 3350 (1996) [arXiv:hep-ph/9603404].
- [49] A. J. Buras, A. Czarnecki, M. Misiak and J. Urban, Nucl. Phys. B **631**, 219 (2002) [arXiv:hep-ph/0203135].
- [50] G. P. Korchemsky and A. V. Radyushkin, Nucl. Phys. B **283**, 342 (1987); I. A. Korchemskaya and G. P. Korchemsky, Phys. Lett. B **287**, 169 (1992).
- [51] S. Moch, J. A. M. Vermaseren and A. Vogt, Nucl. Phys. B **688**, 101 (2004) [arXiv:hep-ph/0403192].
- [52] B. O. Lange, M. Neubert and G. Paz, JHEP **0510**, 084 (2005) [arXiv:hep-ph/0508178].
- [53] B. O. Lange, M. Neubert and G. Paz, arXiv:hep-ph/0504071.
- [54] F. J. Tackmann, Phys. Rev. D **72**, 034036 (2005) [arXiv:hep-ph/0503095].
- [55] M. Neubert, Eur. Phys. J. C **40**, 165 (2005) [arXiv:hep-ph/0408179].

- [56] C. Balzereit, T. Mannel and W. Kilian, Phys. Rev. D **58**, 114029 (1998) [arXiv:hep-ph/9805297].
- [57] C. N. Burrell, M. E. Luke and A. R. Williamson, Phys. Rev. **D69**, 074015 (2004) [arXiv:hep-ph/0312366].
- [58] K. S. M. Lee *et al.*, to appear.
- [59] H. Boos, T. Feldmann, T. Mannel and B. D. Pecjak, arXiv:hep-ph/0504005.
- [60] C. W. Bauer, D. Pirjol, I. Z. Rothstein and I. W. Stewart, Phys. Rev. D **70**, 054015 (2004) [arXiv:hep-ph/0401188].
- [61] T. Feldmann and T. Hurth, JHEP **0411**, 037 (2004) [arXiv:hep-ph/0408188].
- [62] M. Beneke, G. Buchalla, M. Neubert and C. T. Sachrajda, Phys. Rev. D **72**, 098501 (2005) [arXiv:hep-ph/0411171].
- [63] C. W. Bauer, D. Pirjol, I. Z. Rothstein and I. W. Stewart, Phys. Rev. D **72**, 098502 (2005) [arXiv:hep-ph/0502094].